

Nondestructive halide exchange via SN₂-like mechanism for efficient blue perovskite light-emitting diodes

Corresponding Author: Professor Jian-Xin Tang

This file contains all reviewer reports in order by version, followed by all author rebuttals in order by version.

Version 0:

Reviewer comments:

Reviewer #1

(Remarks to the Author)

In this manuscript, the authors proposed a strategy of nondestructive in situ halide exchange through long alkyl chain chloride incorporated CF post-treatment, resulting in highly efficient blue PeLEDs. The different ion exchange processes of IPA and CF post-treatment originate from the difference in solvent destructiveness on perovskite films between IPA and CF. The authors proposed an SN₂-like mechanism to describe the ion exchange process of CF post-treatment. Considering the two kinds of post-treatment seem similar, using such an organic-like mechanism to describe and analyze the ion exchange process in an ionic crystal is not convincing. The innovation of this manuscript is not clear when leaving out the claimed SN₂-like mechanism. The discussion and analysis of improvement on the significant improvement in the optical properties of the CF post-treated films are not sufficient and the expression is not rigorous enough. Specific comments and suggestions are listed below.

1. The authors claimed that only SN₂-like mechanism was clearly temperature-dependent. However, the results in Supplementary Fig.9 do not align with such a statement. Both CF and IPA-treated perovskite films exhibit bluer wavelengths under room temperature than that under low temperature, suggesting the same wavelength tendency with temperature. Moreover, IPA-treated perovskite films exhibit a bluer wavelength compared with CF-treated perovskite films under the same temperature. This result may be caused by the IPA-induced vacancies that enable more Cl to enter the lattice, which has no concern with temperature dependency.

2. In Fig.2e, the activation energy of M2 is 0.99 eV, and energy barrier of TS1 is 1.50 eV. Since 1.0 eV is equivalent to 11600 K, such high theoretical values are not reasonable.

3. In lines 245-248, the authors claimed that 'the larger steric hindrance of Br atoms makes it difficult to replace smaller Cl atoms in the perovskite lattice via CF-based post-treatment'. The ion radius of Br and Cl are 196 pm and 181 pm, respectively, which possesses a tiny difference. Br exists as an ion in perovskite, rather than containing organic groups. The claim of 'larger steric hindrance of Br atoms' can not be acceptable.

4. In Fig.3a, all post-treated perovskite films exhibit similar decay curves, while their PLQYs exhibit obvious differences. The authors should fully discuss such results.

5. The boost in Eb of treated perovskite films means the enhancement of the quantum confinement effect. While the halogen composition change will not lead to the enhancement of the quantum confinement effect. Will the dimension or structure of treated perovskite films have changed after CF post-treatment?

6. The highly efficient blue PeLEDs were achieved based on primitive device structure. In general, the PEDOT:PSS could quench the perovskite film when directly deposit the perovskite film on it. Therefore, I strongly encourage the authors to provide the PLQY of treated perovskite film on the PEDOT:PSS, as well as the light out-coupling efficiency of the device structure in the manuscript, and to provide some discussion on the reasons for achieving the high efficiency.

7. How about the EL spectra stability of blue PeLEDs based on CF-treated perovskite films under high voltages (6-10 V)?

Reviewer #2

(Remarks to the Author)

The manuscript by Kai Zhang et al. proposed a halide exchange strategy for the deep blue perovskite light-emitting diodes (PeLEDs). While halide exchange has proven effective for adjusting PeLED emission colors, it often results in high defect densities because of solvent damage. They proposed a method for halide exchange that avoids damage and achieves high-quality blue perovskites with low trap densities and adjustable bandgaps. This approach involves using a chloroform post-treatment with long alkyl chain chlorides. Experimental and theoretical studies indicate that this method employs a unique SN₂-like ionic exchange mechanism. They insisted that the strategy not only adjusts the bandgaps of perovskites but also prevents the formation of new halogen vacancies. As a result, they achieved highly efficient PeLEDs across various blue wavelengths, with record external quantum efficiencies of 23.6% for sky-blue emission at 488 nm, 20.9% for pure-blue emission at 478 nm, and 15.0% for deep-blue emission at 468 nm. This research represents a major advancement in halide exchange for producing high-performance blue PeLEDs.

This paper insisted the high external efficiency values with the halide exchange method. However, halide exchange materials of butylammonium halide was already used for color change process in a previously reported paper (Adv. Sci. 2022, 9, 2200073). Therefore, it is hard to say that this paper proposed a novel and new strategy for efficient deep blue perovskite light-emitting diodes. Also, considering the big energy barrier between HTL and perovskite (Fig. 4a), the performances reported are questionable. The methods and experimental sections were so poorly described that other researchers may not be able to reproduce the results appropriately. In addition to the chemical perspective, the electrical explanation for the high efficiency is not described well, either.

1. It is necessary to rewrite the experimental section in such detail that future researchers reading this paper will be able to perfectly reproduce the results, including:

- Stirring time and temperature of HTL mixture
- Stirring time and temperature of both perovskite precursor solution and CF post-treatment solution
- Respective thicknesses and deposition rates of TPBi, LiF, Al
- When making perovskite film, which antisolvent was used? Also, antisolvent dripping timing and the amount should be written.
- Exact soaking time of post-treatment solution should be written in the experimental section.
- Power used in the UV-ozone process
- Full names and exact product information (product number, company, specification) of ETA.
- Were PLQY values measured on bare glass or HTL? Also, the intensity, power, and wavelength of excitation light used for PLQY measurement should be provided.
- For perovskite precursor solution, the composition should be described in molar concentrations and ratios for respective chemicals such as PbBr₂, PbCl₂, etc.

2. The authors used CF and IPA for post-treatment solution. Reviewers request to try to use other solvents such as ethanol, butanol, ethyl acetate, chlorobenzene, toluene, xylene, etc. Also, the performance differences (EQE, L_{max}, current density, operational lifespan, color stability (EL vs wavelength with different voltages)) with different solvents should be provided.

3. It is necessary to show the UPS data and energy diagram of HTL (mixture of normal Al₄O₃ aqueous solution and ETA) with different amounts of ETA such as 1,2,3,4,5,6,7,8,9,10 vol.%. Also please show the device performance differences (EQE, L_{max}, current density, operational lifespan, color stability (EL vs wavelength with different voltages)) of distinct HTL-based PeLEDs with different amounts of ETA from 1 to 10 vol.%

4. In Fig. S21, it seems the emission wavelength has changed as operation voltage, so CIE coordination change plot for different operation voltages should be provided (CIE x,y coordinate vs voltage plot) Also, EQE and FWHM plot as a function of voltage should be denoted.

5. The electrical explanation for the high efficiency should be described because there have been many papers showing higher PLQY but lower EQE compared to this paper.

Reviewer #3

(Remarks to the Author)

Blue perovskite light-emitting diodes (PeLEDs) continue to face significant challenges due to the difficulty in achieving high-quality mixed-halide perovskites with wide optical bandgaps. Traditional halide exchange methods, although effective in tuning the emission color of PeLEDs, often result in high defect densities due to solvent erosion. This study presents an innovative strategy for nondestructive in situ halide exchange, aiming to produce high-quality blue perovskites with low trap densities and tunable bandgaps. This paper is achieved through a chloroform post-treatment incorporating long alkyl chain chlorides. Both experimental results and theoretical calculations indicate a unique SN₂-like ionic exchange mechanism with this approach. Unlike conventional halide exchange methods, this strategy not only modulates perovskite bandgaps but also prevents the formation of new halogen vacancies. The nondestructive halide exchange strategy enables the production of efficient PeLEDs across the blue spectral region, achieving record-breaking external quantum efficiencies of 23.6% (sky-blue emission at 488 nm), 20.9% (pure-blue emission at 478 nm), and 15.0% (deep-blue emission at 468 nm). This work represents a significant advancement in the field and provides valuable insights into halide exchange processes for developing high-performance blue PeLEDs.

1. It is mentioned that Cs and halogens are removed during IPA treatment, but the EDS data for Pb ions seems to be

- missing. Additionally, it would be better to compare figure S1 and S2 using the same scale bar for consistency.
2. In Supplementary Fig 5, the XPS data shows inconsistencies in the peak intensity trends for Br and Cl depending on the wavelength of the light. The author needs more explain.
 3. It is stated that a higher Cl ratio reduces defect tolerance; however, figure 3c shows that the VTFL for deep blue is lower than that for pure blue. The author needs more explain.
 4. There are discrepancies between the figures mentioned in the paper and the corresponding descriptions. Please correct these, particularly the reference on line 176 (supplementary fig 2a -> fig 2a) and on line 271 (Supplementary Note 2 -> Supplementary Note 1).
 5. In figure 3(d), it is stated that the shift of the C-N peak in FTIR data is contributed by the coordination interaction between the amine group and the uncoordinated Pb atoms. Given that the amine group of ligands is generally attached to halides of the perovskite frame by coulombic attraction, is there a reason to describe the interaction between the amine group and Pb atoms?

Version 1:

Reviewer comments:

Reviewer #1

(Remarks to the Author)

Authors have performed various experiments for supporting their opinion.

These results and the responses of revision provide the suitable evidences for publications.

In the revised version that have added new data, strengthening the discussion and clarifying reviewers' doubts, consequently I suggest the publication of the revised version.

Reviewer #3

(Remarks to the Author)

The author mostly covered my comments therefore, I recommend this paper be published in natural communications

Open Access This Peer Review File is licensed under a Creative Commons Attribution 4.0 International License, which permits use, sharing, adaptation, distribution and reproduction in any medium or format, as long as you give appropriate credit to the original author(s) and the source, provide a link to the Creative Commons license, and indicate if changes were made.

In cases where reviewers are anonymous, credit should be given to 'Anonymous Referee' and the source.

The images or other third party material in this Peer Review File are included in the article's Creative Commons license, unless indicated otherwise in a credit line to the material. If material is not included in the article's Creative Commons license and your intended use is not permitted by statutory regulation or exceeds the permitted use, you will need to obtain permission directly from the copyright holder.

To view a copy of this license, visit <https://creativecommons.org/licenses/by/4.0/>

Response Letter

We appreciate the valuable comments and suggestions from the editors and reviewers on our research article entitled “Nondestructive halide exchange via S_N2 -like mechanism for efficient blue perovskite light-emitting diodes”. According to these comments and suggestions, we have supplemented corresponding data and necessary discussions in our revised manuscript, which have certainly improved the quality of our work. In the following, we offer the point-by-point responses to the reviewers’ suggestions and comments and show how the manuscript has been revised. All the revisions have been highlighted in red in the revised manuscript. We sincerely hope the revised manuscript is now suitable for publication in Nature Communications. Thank you for your kind attention.

To Reviewer #1:

In this manuscript, the authors proposed a strategy of nondestructive in situ halide exchange through long alkyl chain chloride incorporated CF post-treatment, resulting in highly efficient blue PeLEDs. The different ion exchange processes of IPA and CF post-treatment originate from the difference in solvent destructiveness on perovskite films between IPA and CF. The authors proposed an S_N2 -like mechanism to describe the ion exchange process of CF post-treatment. Considering the two kinds of post-treatment seem similar, using such an organic-like mechanism to describe and analyze the ion exchange process in an ionic crystal is not convincing. The innovation of this manuscript is not clear when leaving out the claimed S_N2 -like mechanism. The discussion and analysis of improvement on the significant improvement in the optical properties of the CF post-treated films are not sufficient and the expression is not rigorous enough. Specific comments and suggestions are listed below.

Response: We sincerely thank the reviewer for these instructive comments. According to these comments, we have supplemented elaborate supporting data and discussion to preclude misunderstandings and enrich our work. We strongly agree with the reviewer that the discussion and analysis of the optical properties of the CF post-processing film were not sufficient, so we specifically revised the relevant content and provided detailed responses to your suggestions, hoping to gain your understanding and support. Although these two post-treatment processes are extremely similar, the distinct results (including photophysical properties and device performance) indicate that they have completely different intrinsic mechanisms. Therefore, our work has explained the differences between these two processing methods from a microstructural perspective, and it has well-matched the corresponding macroscopic results regarding the in-situ processing process and related performance characterizations. It is noteworthy that the ion behavior in the halogen exchange process has certain similarities with the S_N1 and S_N2 reactions in organics, so we hope to help readers understand the process through the “ S_N1 -like” and “ S_N2 -like” models, but it does not mean that these are real organic reactions. The detailed responses are listed below.

1. Comment (Reviewer #1): *The authors claimed that only S_N2 -like mechanism was clearly temperature-dependent. However, the results in Supplementary Fig.9 do not align with such a statement. Both CF and IPA-treated perovskite films exhibit bluer wavelengths under room temperature than that under low temperature, suggesting the same wavelength tendency with temperature. Moreover, IPA-treated perovskite films exhibit a bluer wavelength compared with CF-treated perovskite films under the same temperature. This result may be caused by the IPA-induced vacancies that enable more Cl to enter the lattice, which has no concern with temperature dependency.*

Response: We apologize for any confusion that may have arisen due to the potential lack of clarity in our language expression regarding this part of the content. Hence, we would like to provide the following clarification.

“The authors claimed that only S_{N2} -like mechanism was clearly temperature-dependent. However, the results in Supplementary Fig.9 do not align with such a statement. Both CF and IPA-treated perovskite films exhibit bluer wavelengths under room temperature than that under low temperature, suggesting the same wavelength tendency with temperature.”

Firstly, we'd like to argue with respect that we didn't claim that only S_{N2} -like mechanism was clearly temperature-dependent. We agree with the reviewer that not only S_{N2} -like mechanism exhibits temperature dependence according to experimental results. This is explicitly mentioned in our paper: *“Differently, the IPA-based post-treatment with the same BACl concentration yields blue-shifted emission at 453 and 470 nm at room and low temperatures, respectively, demonstrating its relatively weaker dependence on temperature.”* This suggests that temperature change has an impact on S_{N1} -like mechanism as well. This effect is attributed to the S_{N1} -like mechanism being based on a dissolution-recrystallization process, where the decrease in solubility at low temperatures leads to a reduction in the number of halide vacancies formed, further resulting in a decrease in the number of chlorine ions during the filling process, which is manifested by the spectral differences at room and low temperatures. However, this effect on solubility is limited, and thus IPA post-treatment still produces an obvious blue-shifted emission at low temperature.

Secondly, temperature plays a dominant role in the S_{N2} -like mechanism. There is a larger adsorption energy and halogen exchange barrier in this mechanism, compared to the solubility energy in the S_{N1} -like process. Therefore, the impact of temperature on

the S_{N2} -like mechanism is critical. At room temperature, thermal energy drives the halogen exchange process, resulting in a blue-shifted emission; while at low temperature, this process is prohibited and the spectrum remains almost unchanged, as shown in Fig. 2e. This is consistent with the visualized results of Supplementary Fig. 11. Therefore, compared to the pristine film, the IPA-treated films exhibit blue-shifted spectra at both room and low temperatures, while the CF-treated film only exhibit blue-shifted spectra at room temperature but no significant change at low temperature, indicating that these two processes have different degrees of dependence on temperature. In addition, as the reviewer noted, both CF- and IPA-treated perovskite films exhibit bluer wavelengths under room temperature than that under low temperature, but the underlying mechanisms for this change are distinctly different. The change for the IPA-treated film is due to the slower halide exchange process caused by solubility, while the change for the CF-treated film is caused by the larger energy barrier that prohibits the halide exchange process.

“Moreover, IPA-treated perovskite films exhibit a bluer wavelength compared with CF-treated perovskite films under the same temperature. This result may be caused by the IPA-induced vacancies that enable more Cl to enter the lattice, which has no concern with temperature dependency.”

As the reviewer mentioned, IPA exhibits a bluer wavelength at the same temperature due to more Cl enter the lattice. It is noteworthy that this conclusion presupposes the same temperature, thus it has no relationship with the temperature dependence. The relationship between IPA treatment and temperature has been further explained in the preceding text. Thanks for your comments. To better elucidate this issue, we have expanded the relevant discussion and analysis.

--- *“Differently, the IPA-based post-treatment with the same BA₂Cl concentration yields*

blue-shifted emission at 453 and 470 nm at room and low temperatures, respectively. It is noteworthy that the change in solubility with temperature limits the spontaneous perovskite dissolution process in S_{N1} -like mechanisms at low temperatures, which leads to different PL spectra of IPA post-treated films at room and low temperatures. Nevertheless, this temperature dependence has limited influence and the IPA post-treated film still exhibits a significant blue-shifted PL spectrum at low temperature.”

(Page 10, Line 3-10)

2. Comment (Reviewer #1): *In Fig.2e, the activation energy of M2 is 0.99 eV, and energy barrier of TS1 is 1.50 eV. Since 1.0 eV is equivalent to 11600 K, such high theoretical values are not reasonable.*

Response: Thanks for this valuable comment, which has encouraged us to think more deeply. However, there is an essential difference between eV and Kelvin, which is not suitable for the comparison through simple conversion in real experiments.

Firstly, according to the derivation of the formula $E=k_B T$, 1 eV is indeed equivalent to 11,600 K, but the use of this formula requires the following conditions:

1. **Thermal Equilibrium:** The system should be in thermal equilibrium, meaning the particles follow the Boltzmann distribution at a uniform temperature T.
2. **High-Temperature or Classical Regime:** The approximation works well when the temperature is high enough that thermal energy $k_B T$ is much greater than the energy spacing between quantum states. In this regime, quantum effects are negligible, and the system behaves classically.
3. **Systems with Sufficient Degrees of Freedom:** For systems with multiple degrees of freedom, this relationship can be extended.
4. **Weakly Interacting Particles:** The approximation $E=k_B T$ holds for systems where

particles are weakly interacting, such as in an ideal gas, where interactions between particles are minimal.

In essence, $E=k_B T$ is most suitable for classical systems at high temperatures, in thermal equilibrium, and with weakly interacting particles. However, the simple relation $E=k_B T$ might not accurately describe the energy distribution in materials with strong interactions, such as solids or liquids. In addition, when $k_B T$ is smaller than the energy spacing between quantum states, this approximation breaks down, and quantum statistical mechanics is required. In summary, the formula is not applicable to this study system.

Secondly, the ion migration barrier obtained from kinetic simulations cannot be directly converted into a certain temperature. However, the relationship between the migration barrier and temperature can be used to predict ion migration behavior at different temperatures. The ion migration barrier represents the energy that an ion must overcome to move from one site to another in a material. This value, is an intrinsic property that does not change with temperature. The actual temperature T affects the ability of ions to surmount this energy barrier: the higher the temperature, the more thermal energy the ions acquire, making it easier for them to overcome the barrier and thus accelerate their migration. The process can be described by Arrhenius equation:

$$D = D_0 \exp\left(-\frac{E_a}{k_B T}\right)$$

where D is the diffusion coefficient, D_0 is the pre-exponential factor, E_a is the ion migration barrier, k_B is the Boltzmann constant, and T is the absolute temperature. Although the E_a can be precisely obtained through simulation, the D usually requires experimental determination or more complex calculations. It is related to the material's microstructure and ion species, and accurately determining D is crucial for extrapolating simulation results to actual temperatures. In addition, kinetic simulations

are often conducted under idealized and simplified conditions, whereas in actual environments, materials may contain defects, impurities, grain boundaries, etc., and the actual migration energy barriers may be slightly different. In summary, the migration barrier from simulations helps predict how ion mobility changes with temperature, and thus predicts ion migration behavior under actual operating conditions, but it doesn't convert directly into a specific temperature.

Additionally, we have carefully and thoroughly reviewed our calculation process and noticed that our computational model might contain reaction pathways with lower energy barriers. Accordingly, we revised this section by supplementing DFT calculations with improved models. As shown in Figure 2c, the halide ion exchange process changes from intramolecular rotation to intramolecular translation. The corresponding barrier decreases from 1.5 eV to 0.32 eV. Compared to the activation energy of 1.02 eV for M2 (Figure 2e), the lower barrier in the transition state probably indicates that the chlorine adsorption process determines the exchange rate in S_N2 -like mechanism. For this issue, we have revised and added several sentences for better explanation.

--- *“The ion migration pathway is simulated by using transition state theory (Fig. 2c), where molecular internal translation results in an intermediate structure with the coexistence of Br and Cl ions at the original lattice site.”* (Page 9, Line 7-9)

--- *“In comparison, the S_N2 -like mechanism starts with a high activation energy 1.02 eV to form the intermediate M2, corresponding to the surface adsorption of Cl atoms. Then, the formation of the transition state TS1 requires a barrier of 0.32 eV, necessitating suitable temperature to initiate the halide exchange process, which aligns with the strong temperature dependence observed for the CF-based post-treatment.”* (Page 10, Line 21-25)

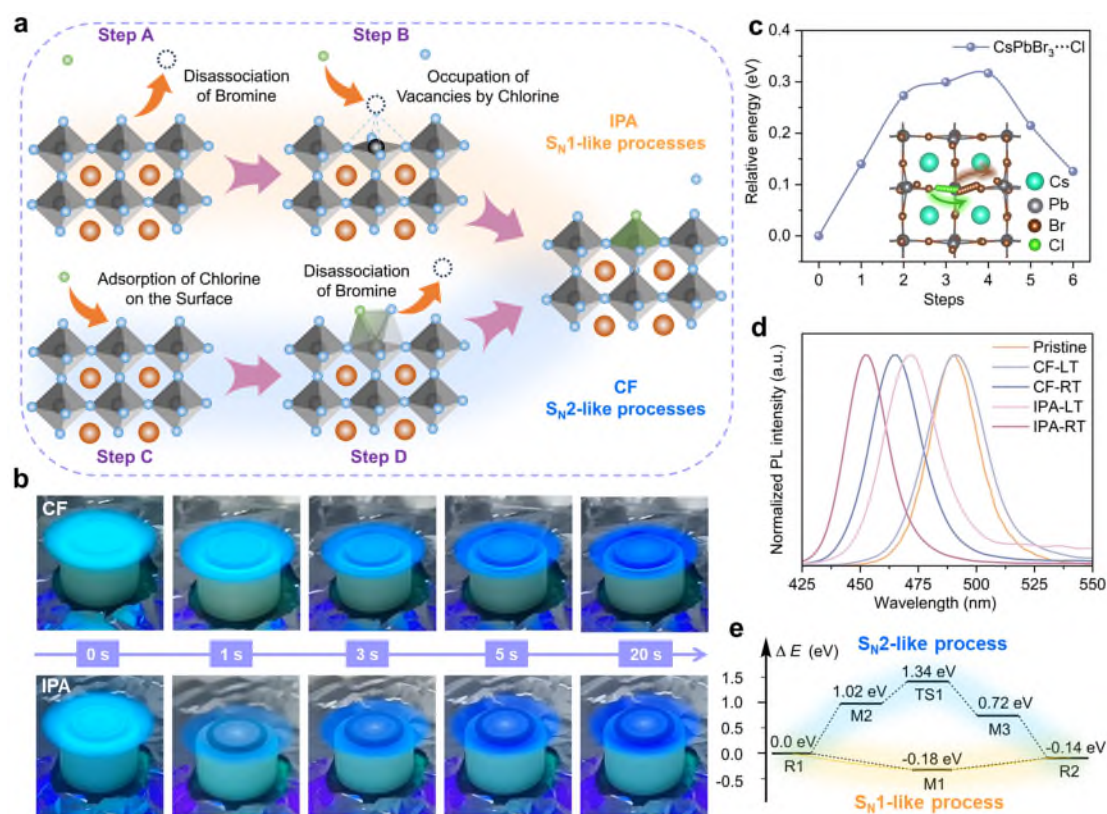
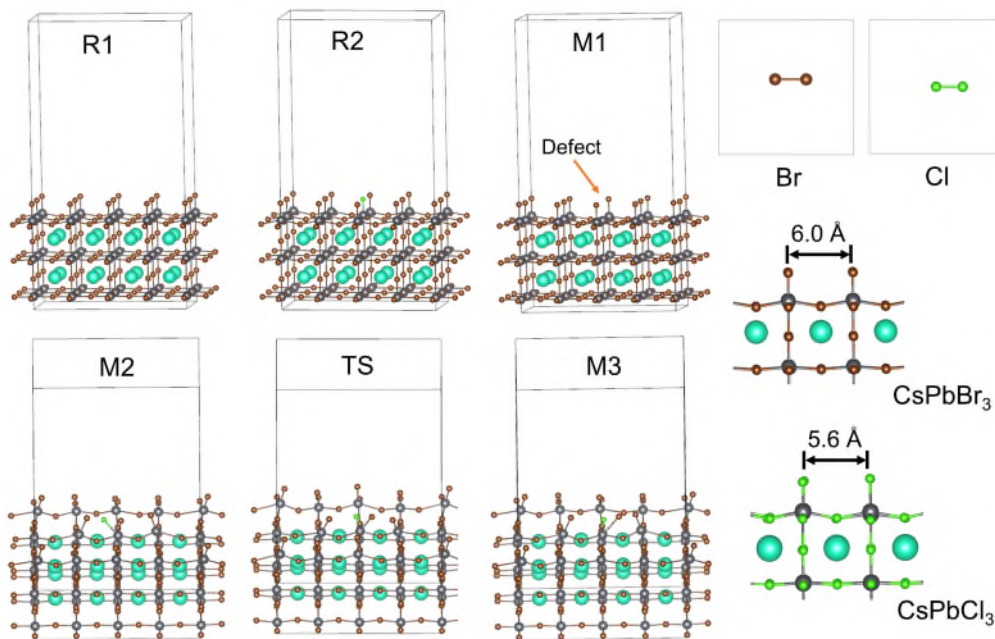


Fig. 2 Underlying mechanism of halogen ion exchange. **a** Schematics of ion exchange reactions based on the S_N1 -like mechanism (IPA post-treatment) and the S_N2 -like mechanism (CF post-treatment). **b** Real-time fluorescence monitoring images during IPA and CF in-situ post-treatment. **c** Relative energy landscapes for ion migration pathway in S_N2 -like halogen exchange process. The inset shows the theoretical models of the perovskite lattices during the exchange process. **d** Low-temperature (LT) and room-temperature (RT) post-treatment of PL spectra of CF and IPA solvents. **e** Potential energy profiles in halogen ion exchange pathways based on S_N1 -like and S_N2 -like mechanisms. (R1: reactants, $\text{CsPbBr}_3 + \text{Cl}$. R2: product, $\text{CsPbBr}_2\text{Cl} + \text{Br}$. Intermediate for S_N1 -like process: M1: surface defects of Br, CsPbBr_2 -defect+Br+Cl. Intermediate for S_N2 -like process: M2: Cl adsorbed in crystal surface, $\text{CsPbBr}_3 \cdots \text{Cl}$; M3: Br adsorbed in crystal surface, $\text{CsPbBr}_2\text{Cl} \cdots \text{Br}$; TS1: transition states, $\text{CsPbBr}_2 \cdots \text{Br} \cdots \text{Cl}$)



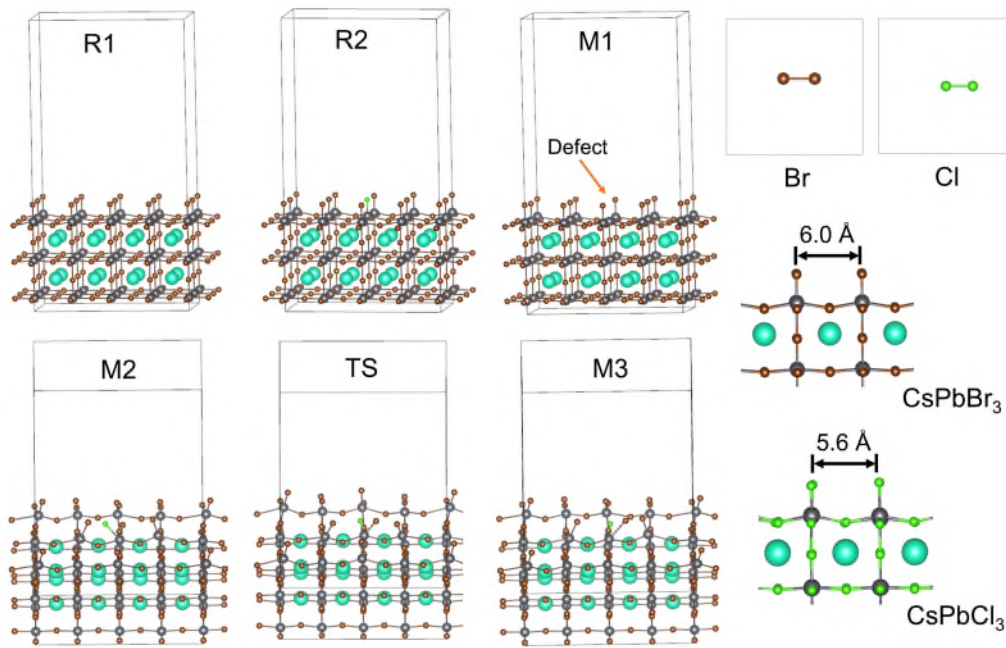
Supplementary Fig. 12. The crystal structures corresponding to different states in theoretical simulations. (R1: reactants, $\text{CsPbBr}_3 + \text{Cl}$. R2: product, $\text{CsPbBr}_2\text{Cl} + \text{Br}$. Intermediate for $\text{S}_{\text{N}}1$ -like process: M1: surface defects of Br, $\text{CsPbBr}_2\text{-defect} + \text{Br} + \text{Cl}$. Intermediate for $\text{S}_{\text{N}}2$ -like process: M2: Cl adsorbed in crystal surface, $\text{CsPbBr}_3 \cdots \text{Cl}$; M3: Br adsorbed in crystal surface, $\text{CsPbBr}_2\text{Cl} \cdots \text{Br}$; TS1: transition states, $\text{CsPbBr}_2 \cdots \text{Br} \cdots \text{Cl}$.)

3. Comment (Reviewer #1): *In lines 245-248, the authors claimed that ‘the larger steric hindrance of Br atoms makes it difficult to replace smaller Cl atoms in the perovskite lattice via CF-based post-treatment’ . The ion radius of Br and Cl are 196 pm and 181 pm, respectively, which possesses a tiny difference. Br exists as an ion in perovskite, rather than containing organic groups. The claim of ‘larger steric hindrance of Br atoms’ can not be acceptable.*

Response: We apologize for any misunderstanding the reviewer may have regarding the issue due to our insufficiently comprehensive and rigorous discussion. According

to our computational results, the bond lengths between adjacent Pb atoms in CsPbBr₃ and CsPbCl₃ crystals are 6.0 Å (Pb-Br-Pb) and 5.6 Å (Pb-Cl-Pb), respectively, as shown in Supplementary Fig. 12. The ion radius of Cl and Br are 1.96 Å and 1.81 Å, respectively. In the S_N2-like process, compared to the adsorption process of Cl atoms on the surface of CsPbBr₃ crystals (1.81/6.0), the larger size of Br atoms and the smaller interstitial space in CsPbCl₃ (1.96/5.6) result in a higher adsorption energy for Br atoms, making it difficult to replace Cl atoms in CsPbCl₃ lattice at room temperature. However, this slightly increased adsorption energy can be overcome by raising the temperature, as shown in Supplementary Fig. 13, where Br atoms can replace Cl atoms in the perovskite lattice under heating conditions. The relevant discussion has been revised.

--- *“Additionally, unlike IPA-based post-treatment, BAbR-incorporated CF solution does not induce a redshift spectrum at room temperature (Supplementary Fig. 13). Compared to the exchange process of substituting Cl for Br atoms, the substitution of Br for Cl atoms has a higher activation energy barrier (Supplementary Fig. 14), due to the increased ionic radius (from 1.81 Å of Cl to 1.96 Å of Br) and the reduced interstitial space (from 6.0 Å in CsPbBr₃ to 5.61 Å in CsPbCl₃) (Supplementary Fig. 12), which inhibits the halide exchange process at room temperature.”* (Page 11, Line 1-8)



Supplementary Fig. 12. The crystal structures corresponding to different states in theoretical simulations.

4. Comment (Reviewer #1): *In Fig.3a, all post-treated perovskite films exhibit similar decay curves, while their PLQYs exhibit obvious differences. The authors should fully discuss such results.*

Response: We thank the reviewer for the insightful comment and suggestion. To verify the accuracy of our tests, we examined the post-treated films under different test parameters, as shown in the Fig. R1. All the post-treated films exhibited similar attenuation curves, which validates the reliability and reproducibility of our data. For the issue that the reviewer mentioned, we offer the following explanation:

It's widely accepted that defect passivation is the main reason for the increased TRPL lifetimes and PLQYs of perovskite films. Compared to the pristine perovskite film, the BA ligand and halide ions in the CF post-treatment process exhibit effective defect passivation for perovskite films (Fig. 3c and 3d), which is beneficial for eliminating

non-radiative recombination channels at the perovskite grain boundaries and increasing the sites for radiative recombination. Therefore, the CF post-treated films show increased lifetimes and radiative recombination rates, as well as reduced non-radiative recombination rates (Fig. 3a and 3b).

However, as the proportion of chlorine increases to enlarge the bandgaps, the increased trapping states with deeper energy levels in bluer perovskite films leads to more serious localized charge trapping (J. Am. Chem. Soc. 2018, 140, 17760), which indicates the reduced defect tolerance, matching well with the results in in Fig. 3b and 3c. Different from the shallow-level traps in the perovskite films with less chlorine, deep-level traps prohibit de-trapping process. It's well known that the PL lifetime is the rate of luminescence intensity decays over time after the material is excited by light, which describes the time required for electrons to return from the excited state to the ground state. The principle of PL lifetime testing relies on the excitation of the sample with a pulsed laser and the real-time detection of the emission signal. Under high-intensity excitation at the initial stage of TRPL measurements, the deep-level traps in bluer perovskite films are filled with charges and no longer capture charges after the excitation. On this condition, all the perovskite films still exhibit similar TRPL curves, suggesting that the trap states in bluer perovskite films are higher at ground state. Different from TRPL lifetime, PLQY is defined as the ratio of the number of photons emitted by the luminescent material to the number of absorbed photons. Hence, the bluer perovskite films with increased deep-level traps and reduced defect tolerance suffer from more serious non-radiative recombination, featuring greatly decreased PLQYs, which represents a critical factor for the inferior performance of deep-blue PeLEDs nowadays. According to these discussions, we have the conclusion that it's unreasonable to predict the PLQYs of the perovskite films with different bandgaps (or

halogen molar ratios) just through their TRPL lifetimes. By summarizing the results from many literatures, red, green, and blue perovskite films with similar PLQYs may feature distinct TRPL lifetimes even with orders of magnitude difference.

Accordingly, we have supplemented relevant discussion:

--- *“Compared to the control perovskite film, the sky-, pure-, and deep-blue samples yield much improved PLQYs of 83.8%, 72.1%, and 58.0%, respectively (Supplementary Fig. 15). Notably, although all the post-treated perovskite films exhibit similar TRPL curves, the increased deep-level traps and reduced defect tolerance induced by higher Cl/Br ratio greatly degrade the PLQYs of the perovskite films with wider bandgaps.”*

(from Page 11, Line 23 to Page 12, Line 4)

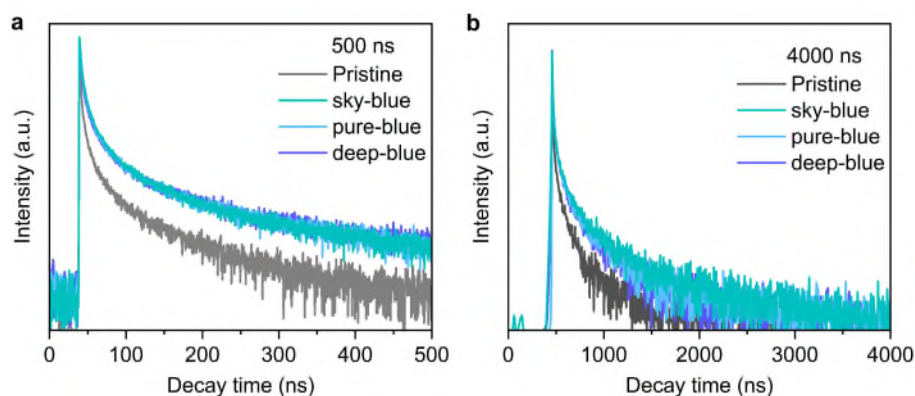


Fig. R1. TRPL spectra of pristine and post-treated perovskite films at (a) 500 ns and (b) 4000 ns.

5. Comment (Reviewer #1): *The boost in E_b of treated perovskite films means the enhancement of the quantum confinement effect. While the halogen composition change will not lead to the enhancement of the quantum confinement effect. Will the dimension or structure of treated perovskite films have changed after CF post-treatment?*

Response: We thank the reviewer for raising these important points. We strongly agree with the reviewer that enhanced quantum confinement effect can lead to an increase in E_b . However, the increase in E_b does not necessarily originate from the enhancement in quantum confinement effect. The halogen composition change can also lead to an increase in E_b ; please refer to the following literature: J. Phys. Chem. Lett. 2015, 6, 23, 4688-4692; J. Phys.: Condens. Matter 1996, 8, 5953; Solid State Commun. 2003, 127, 619-623. Moreover, the defect densities in perovskite films have an impact on their E_b as well. More crystal defects can induce intenser charge trapping and reduce the E_b of perovskite films.

Considering the non-destructive post-treatment of our strategy, which is evidenced by the EDS mapping (Supplementary Fig. 1 and 2), we excluded the factor of the changes in the dimension and structure of treated perovskite films.

6. Comment (Reviewer #1): *The highly efficient blue PeLEDs were achieved based on primitive device structure. In general, the PEDOT:PSS could quench the perovskite film when directly deposit the perovskite film on it. Therefore, I strongly encourage the authors to provide the PLQY of treated perovskite film on the PEDOT:PSS, as well as the light out-coupling efficiency of the device structure in the manuscript, and to provide some discussion on the reasons for achieving the high efficiency.*

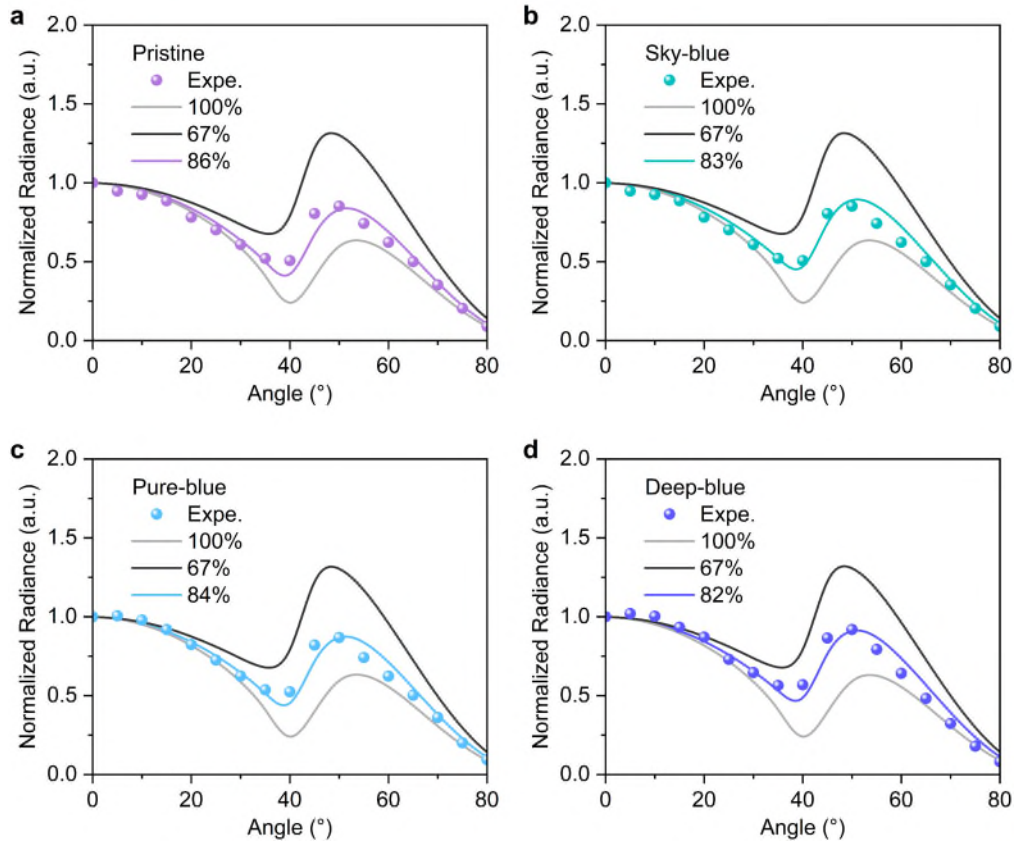
Response: We sincerely thank the reviewer for suggesting us elucidate the reasons for high device efficiency. The nature of the underlying substrate surface profoundly affects the perovskite crystallization, which leads to difference photophysical properties of perovskite films based on diverse substrates. To ensure the effectiveness of our results, the PLQY results in our manuscript were exactly obtained from the perovskite films as prepared on PEDOT:PSS substrate. One sentence has been revised in the **Methods**

section.

--- “*The absolute photoluminescence quantum yields (PLQYs) of blue perovskite films on PEDOT:PSS substrate were measured under nitrogen atmosphere at room temperature through a C9920-02G type fluorescence spectrophotometer (HAMAMASTU, Japan) with an integrating sphere excited at 365 nm.*” (from Page 19, Line 26 to Page 20, Line 4)

As the reviewer mentioned, our devices were achieved based on primitive device structure. **In the following, we provide the discussion on the device light out-coupling to unravel the reasons for the high efficiency of blue PeLEDs:**

Firstly, we measured the horizontal transition dipole moments (TDMs) Θ of the perovskite films. As shown in Supplementary Fig. 22, the pristine perovskite film exhibits a high Θ value up to 86%, while the sky-, pure-, and deep-blue films feature the similar Θ values of 83%, 84%, and 82%, respectively. As widely reported, such high Θ is beneficial for improving the light extraction efficiency of devices, thereby improving the external quantum efficiencies of blue PeLEDs.



Supplementary Fig. 22. Horizontal transition dipole moments measurement of perovskite films. Angle-dependent PL measurements of (a) pristine (Θ : 86%), (b) sky-blue (Θ : 83%), (c) pure-blue (Θ : 84%), and (d) deep-blue (Θ : 82%) perovskite film. The orientation of TDMs in the quasi-2D film is quantified as the ratio of horizontal TDMs, denoted by Θ .

Secondly, we utilized finite-difference time-domain (FDTD) simulation to qualitatively investigate the light out-coupling. According to conventional LED models, large portion of light is trapped inside device due to various channels of optical loss, such as waveguide mode, substrate mode, and metal surface plasmonic polaritons (SPP) mode. Importantly, the waveguide mode light loss is highly sensitive to the thickness of luminescent film. Reducing the thickness of perovskite film is favorable for mitigating the light waveguide. In our work, the thicknesses of blue perovskite films are less than

20 nm, which are much smaller than those of conventional LEDs, so we speculate that the light extraction efficiencies of our devices are higher than those of conventional LEDs. To demonstrate the advantage of perovskite thin film (~ 20 nm), we constructed device models based on the perovskite films with medium thickness (60 nm) and high thickness (100 nm) and simulate their light out-coupling by FDTD method (Fig. R2.). Apparently, for all the sky-, pure-, and deep-blue devices, reducing the thickness of perovskite films can effectively boost the light out-coupling from device inside to air. Therefore, based on the post-treated perovskite films with improved PLQYs, we can attribute the outstanding efficiency to the high device light out-coupling, which originates from the high horizontal transition dipole moments and small thicknesses of perovskite films. For this issue, we have supplemented some discussion:

--- *“It’s noteworthy that the high EQEs of these blue PeLEDs rely on the good horizontal dipole orientation of the perovskite films. By fitting the angle-dependent PL test data, the horizontal transition dipole moments (TDMs) Θ of sky-, pure-, and deep-blue perovskite films reaches 83%, 84%, and 82%, respectively, which is higher than those of ideally isotropic emitters (67%) (Supplementary Fig. 22). A higher Θ is favorable for light extraction from the internal perovskite films to air. Compared to 86% of the pristine film, the similar Θ values in the post-treated films support the reliability of the anti-solvent non-destructive post-treatment strategy. Moreover, the small thicknesses of perovskite films may suppress the waveguide light loss within devices, further boosting the device light out-coupling.”* (Page 15, Line 13-22)

We’re really sorry that we cannot provide a specific light out-coupling efficiency of the device structure as the reviewer recommended, because the calculation of this out-coupling efficiency highly depends on the precise refractive index, film morphology,

film roughness, and film thickness measurements of each functional layers. Considering these rigorous and unattainable requirements, we supplemented the light field distribution simulation by FDTD instead. It's worth noting that the FDTD simulation come from the view of optical theory, which is intended to unveil the potential factor for the high efficiencies of our devices. The finding from the FDTD results doesn't mean that the perovskite films should be prepared as thin as possible for higher light out-coupling. Reducing the film thickness blindly is more likely to cause device current leakage under bias. Actually, the film coverage, phase distribution, and electrical property of perovskite film, which all have critical impact on the device performance, are highly related to perovskite film thickness. A high device efficiency relies on the comprehensive regulation for perovskite film.

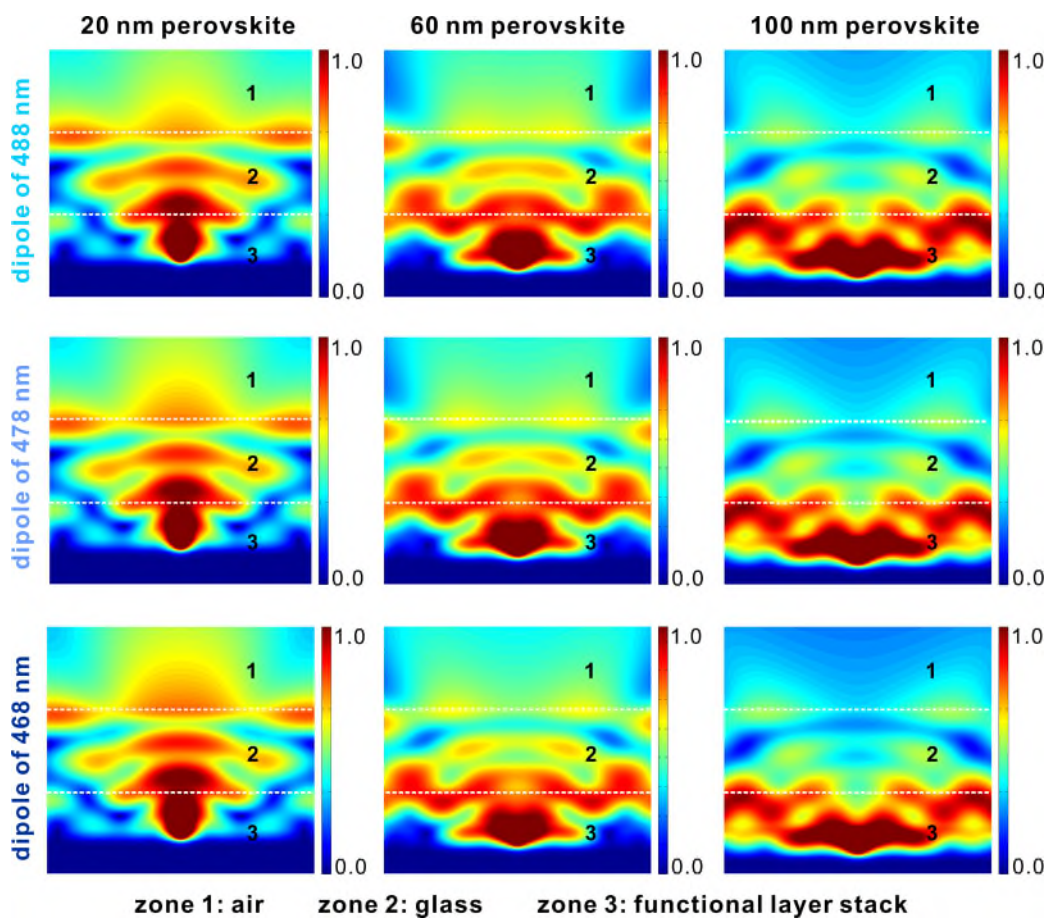


Fig. R2. FDTD simulations of sky-, pure-, and deep-blue PeLEDs based on perovskite films with the thicknesses of 20 nm, 60 nm, and 100 nm.

Apart from the above factors, improving the charge transport balance factor is also critical for high efficiency. As we responded to Reviewer 2 # Comment 3, we have supplemented the UPS measurements on the ETA-modified PEDOT:PSS used in our work. The ETA modification, which is inspired by our previous works, has been demonstrated to reduce the charge transport barrier from HTL to perovskite layers, thereby facilitating the charge balance inside perovskite films and improve the recombination efficiency. The corresponding data is shown in Supplementary Fig. 19,20 and relevant discussion has been added in our revised manuscript:

--- *“The device energy level diagram is schematically depicted in Fig. 4a, where the valence and conduction bands of perovskite film were characterized through ultraviolet photoelectron spectroscopy (UPS) and Tauc plot analysis of the absorption spectra (Supplementary Fig. 17). The energy levels of PEDOT:PSS layers with varying ETA doping ratios were determined by the UPS spectra in Supplementary Fig. 19,20, indicating that ETA modification facilitates the hole transport by reducing the energy barrier from PEDOT:PSS to perovskite films.”* (Page 14, Line 14-21)

In summary, the high efficiency of our blue PeLEDs can be ascribed to the collaborative improvement of inside radiative recombination, charge transport balance, and device light out-coupling.

7. Comment (Reviewer #1): *How about the EL spectra stability of blue PeLEDs based on CF-treated perovskite films under high voltages (6-10 V)?*

Response: Thank the reviewer for the question on EL spectral stability. We apologize for any misunderstanding caused by our incorrect figure notes. As an example, Fig. R2

shows that the erroneous notes used a step size of 0.2 V (the data on the left from Origin software), whereas the corresponding step size that we chose for drawing from the source data should have been 0.4 V (the data on the right from Excel). We have corrected this error, as shown in the revised Supplementary Fig. 26.

In terms of the missing EL spectral stability under high voltages, we provide the following explanation:

The EL spectral stability is a critical factor in evaluating device performance. Typically, this stability is measured by the shift in the EL spectrum from the turn-on voltage to the voltage at maximum luminance (Nature 2024, 631, 73-79; Nature Electronics 2024, 7, 487-496). It is well-established that after a device reaches its peak brightness, subsequent decay occurs due to damage from high current densities. In PeLEDs based on perovskite thin films, elevated drive voltages can damage the emissive layers due to the high electric field. During testing, once a device reached its maximum brightness and began to degrade, we ceased measurements. Collecting EL spectra from degraded devices provides no useful data. Therefore, our stability measurements report EL spectra only during normal operation, up to the point where the device achieves maximum brightness.

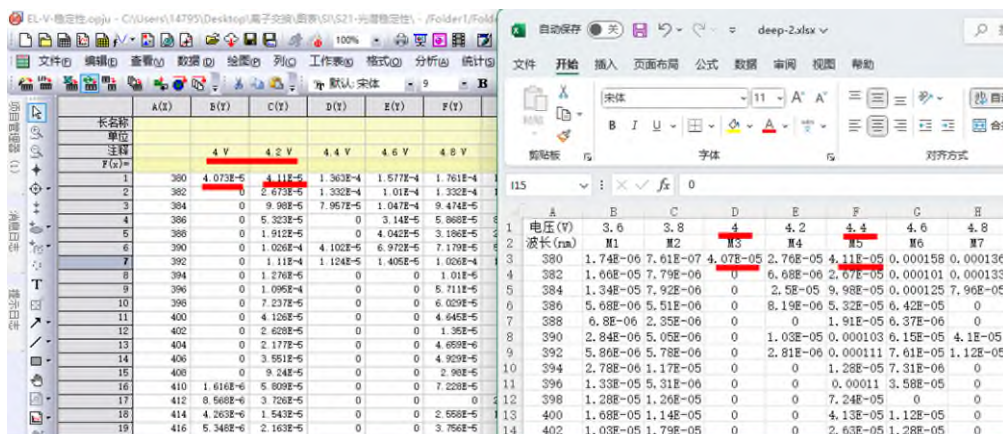
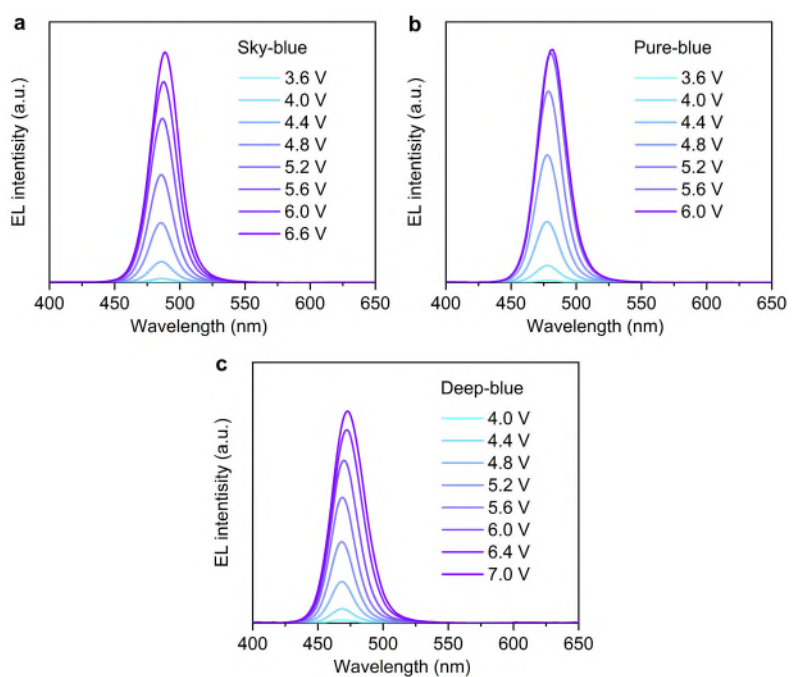


Fig. R2. A screenshot of part of the original data on the stability of the EL spectrum.



Supplementary Fig. 26. EL spectra of the sky-, pure-, and deep-blue devices with CF post-treatment under various driving voltages.

To Reviewer #2:

This paper insisted the high external efficiency values with the halide exchange method. However, halide exchange materials of butylammonium halide was already used for color change process in a previously reported paper (Adv. Sci. 2022, 9, 2200073). Therefore, it is hard to say that this paper proposed a novel and new strategy for efficient deep blue perovskite light-emitting diodes. Also, considering the big energy barrier between HTL and perovskite (Fig. 4a), the performances reported are questionable. The methods and experimental sections were so poorly described that other researchers may not be able to reproduce the results appropriately. In addition to the chemical perspective, the electrical explanation for the high efficiency is not described well, either.

Response: We sincerely appreciate the reviewer's valuable comments on our work. Firstly, we have also taken note of this paper (Adv. Sci. 2022, 9, 2200073); however, this study employs butanol as a treatment solvent, which led to the etching of the perovskite crystals, further resulting in reduced luminescence efficiency. This etching effect is similar to that of isopropanol. In our work, we were also unable to fabricate high-performance devices using either isopropanol or butanol, which is determined by the inherent properties (perovskite erosion) of these solvents. Secondly, the novelty of our strategy basically lies in the non-destructive halogen exchange process. We hope to provide a reference for more researchers by designing this scheme (long alkyl chain ammonium salts and antisolvents), rather than being limited to individual additives. Therefore, butyl ammonium salt was used as the primary material to verify the feasibility of our non-destructive halogen exchange strategy. Thirdly, we modified PEDOT:PSS by using ethanolamine (ETA) according to our previous works, while we neglected the effect of ETA modification on the energy barrier in our original manuscript. The energy

level of PEDOT:PSS in the original manuscript refers to the results reported in relevant literatures. We are really sorry for our carelessness. According to the reviewer's suggestions, we measured the energy level of the modified PEDOT:PSS films, which showed a deeper HOMO level from the 5.2 eV to 5.7 eV after ETA modification, effectively reducing the energy barrier between the HTL and perovskite films. Apart from that, we also supplemented the investigation on the optical out-coupling of our devices, which provides further explanations for high device efficiency.

Finally, we also thank the reviewer for the comment on the experimental details of our manuscript. Accordingly, we have improved the relevant **Methods** section to ensure that other researchers can replicate our results as accurately as possible. Please see the detailed point-by-point response below.

1. Comment (Reviewer #2): *It is necessary to rewrite the experimental section in such detail that future researchers reading this paper will be able to perfectly reproduce the results, including:*

-Stirring time and temperature of HTL mixture

-Stirring time and temperature of both perovskite precursor solution and CF post-treatment solution

-Respective thicknesses and deposition rates of TPBi, LiF, Al

-When making perovskite film, which antisolvent was used? Also, antisolvent dripping timing and the amount should be written.

-Exact soaking time of post-treatment solution should be written in the experimental section.

-Power used in the UV-ozone process

-Full names and exact product information (product number, company, specification)

of ETA.

-Were PLQY values measured on bare glass or HTL? Also, the intensity, power, and wavelength of excitation light used for PLQY measurement should be provided.

-For perovskite precursor solution, the composition should be described in molar concentrations and ratios for respective chemicals such as PbBr₂, PbCl₂, etc.

Response: We sincerely thank the reviewer for careful reading. We have refined these aspects and hope that it will help other researchers reproduce our experimental results. Regarding these points as the reviewer raised, we have provided response one by one below. The revised experimental methods and details are attached at the end.

-Stirring time and temperature of HTL mixture

We stirred the mixed solution of PEDOT:PSS and ETA for 15 min at room temperature and then stored it at 2-5°C for use.

-Stirring time and temperature of both perovskite precursor solution and CF post-treatment solution

The perovskite precursor solution was stirred at 40°C for 12 hours, and the CF post-treatment solution was stirred at room temperature for 2 hours.

-Respective thicknesses and deposition rates of TPBi, LiF, Al

TPBi was deposited at a rate of 2 Å/s to a thickness of 40 nm. LiF was deposited at a rate of 0.1 Å/s to a thickness of 1 nm. Al was deposited at a rate of 5 Å/s to a thickness of 100 nm.

-When making perovskite film, which antisolvent was used? Also, antisolvent dripping timing and the amount should be written.

No antisolvent treatment was used during the preparation of the perovskite film.

-Exact soaking time of post-treatment solution should be written in the experimental section.

During the post-treatment process, 60 μL of CF solution was spin-coated onto the pristine films at 5500 rpm for 1s.

-Power used in the UV-ozone process

The UV-ozone process was performed using a PSD Pro system from *Novascan* at room temperature for 20 minutes. The power is the default of this equipment.

-Full names and exact product information (product number, company, specification) of ETA.

ETA, short for ethanolamine, was used as a 500 ml reagent from Thermo Scientific, with the product number N281001.

-Were PLQY values measured on bare glass or HTL? Also, the intensity, power, and wavelength of excitation light used for PLQY measurement should be provided.

The PLQY values were measured on the HTL. The wavelength of the excitation light used for PLQY measurement is 365 nm. The intensity of the excitation light is around 6.0×10^7 (arbitrary unit). The power of the output is the default of this equipment.

-For perovskite precursor solution, the composition should be described in molar concentrations and ratios for respective chemicals such as PbBr_2 , PbCl_2 , etc.

The pristine perovskite precursor solution was prepared by dissolving PbBr_2 (0.037 M), PbCl_2 (0.062 M), CsBr (0.141 M), *p*-F-PEABr (0.049 M), FABr (0.016 M), and KBr (0.025 M) in DMSO solvent. For the CF post-treatment solution, $\text{BABr}_{0.7}\text{Cl}_{0.3}$ (0.004 M), $\text{BABr}_{0.4}\text{Cl}_{0.6}$ (0.004 M), and $\text{BABr}_{0.1}\text{Cl}_{0.9}$ (0.004 M) were added into the CF solvent to prepare sky-, pure-, and deep-blue perovskite films, respectively.

We have revised the corresponding descriptions in the Methods section. The revision is shown below (Page 18, highlighted in red):

--- “Ethanolamine(ETA) was purchased from Thermo Scientific and its product number

is N281001.”

--- “The pristine perovskite precursor solution was prepared by dissolving PbBr_2 (0.037 M), PbCl_2 (0.062 M), CsBr (0.141 M), $p\text{-F-PEABr}$ (0.049 M), FABr (0.016 M), and KBr (0.025 M) in DMSO solvent, which was stirred for 12 h at 40°C. For the CF post-treatment solution, $\text{BABr}_{0.7}\text{Cl}_{0.3}$ (0.004 M), $\text{BABr}_{0.4}\text{Cl}_{0.6}$ (0.004 M), and $\text{BABr}_{0.1}\text{Cl}_{0.9}$ (0.004 M) was added into the CF solvent at room temperature for 2 h to prepare sky-, pure-, and deep-blue perovskite films, respectively. The blue PeLEDs were fabricated with a structure of ITO (150 nm)/PEDOT:PSS (30 nm)/Perovskite (20 nm)/TPBi (45 nm)/LiF (1 nm)/Al (100 nm). The patterned ITO-coated glass substrates were cleaned sequentially by ultrasonication in detergent solution, deionized water, ethanol, and isopropanol each for 7 min, respectively, and then dried at 90 °C for 120 min in an oven. Before the deposition of PEDOT:PSS, the ITO substrates were treated in a UV-ozone cleaner (Novascan PSD Pro system) for 20 min at room temperature. The PEDOT:PSS aqueous solution was mixed with 4 vol.% ETA, stirred at room temperature for 15 minutes, and then store at 2-5 °C. The modified PEDOT:PSS was spin-coated in the air onto ITO at 4000 rpm for 40 s, followed by thermal annealing at 140 °C for 15 min. The perovskite films were formed by spin-coating the precursor onto PEDOT:PSS layer at 4000 rpm for 60 s, followed by annealing at 70 °C for 5 min. The post-treatment process was completed by spin-coating the CF solution of 60 μL at 1s onto the perovskite layer at 5500 rpm for 50 s, without the need for annealing. After preparing the perovskite films, the TPBi, LiF, and Al electrode were successively deposited in a thermal evaporator at a pressure less than 2×10^{-6} Torr. The deposition rate and layer thickness were monitored with a quartz crystal oscillator. TPBi was deposited at a rate of 2 Å/s to a thickness of 40 nm. LiF was deposited at a rate of 0.1 Å/s to a thickness of 1 nm. Al was deposited at a rate of 5 Å/s to a thickness of 100 nm. The active emitting

area of PeLEDs was 0.1 cm^2 as determined by the overlap between ITO and Al electrodes. The hole-only devices were fabricated with an architecture of ITO/PEDOT:PSS/perovskite/CBP/MoO_x/Al.”

--- “The absolute photoluminescence quantum yields (PLQYs) of blue perovskite films on PEDOT:PSS substrate were measured under nitrogen atmosphere at room temperature through a C9920-02G type fluorescence spectrophotometer (HAMAMASTU, Japan) with an integrating sphere excited at 365 nm. The intensity of the excitation light is around 6.0×10^7 (arbitrary unit).”

2. Comment (Reviewer #2): *The authors used CF and IPA for post-treatment solution. Reviewers request to try to use other solvents such as ethanol, butanol, ethyl acetate, chlorobenzene, toluene, xylene, etc. Also, the performance differences (EQE, Lmax, current density, operational lifespan, color stability (EL vs wavelength with different voltages)) with different solvents should be provided.*

Response: We thank the reviewer for this thought-provoking suggestion. We used CF and IPA as post-treatment solvents because the former is a typical antisolvent with high solubility, while the latter, as a conventional post-treatment solvent, has a significant erosive effect on perovskites. Based on these properties, other solvents suggested by the reviewer can also be categorized into these two types. Similar to CF, ethyl acetate (EA), chlorobenzene (CB), toluene (Tol), and xylene (Xyl) can effectively protect perovskite films as antisolvents, despite notable differences in solubility. Similar to isopropanol (IPA), ethanol (EtOH) and butanol (BuOH) have some solubility for perovskite films. Based on these classifications, we fabricated the corresponding devices and discussed them individually.

For EA, CB, Tol, and Xyl, although these antisolvents effectively protected the

perovskite films, their solubility for chloride salts was significantly lower than CF. As shown in Figure R3, these solvents have low solubility for BACl, especially EA, which is almost completely insoluble for BACl salt. Therefore, we selected CB, Tol, and Xyl for further investigation. Due to the low solubility of chloride salts, the perovskite films and devices were limited to the sky-blue spectral range. As shown in Supplementary Fig. 29, CB-, Xyl-, and Tol-treated devices exhibited peak EQEs of 20.12%, 19.01%, and 16.77%, respectively, which were significantly higher than 13.53% of the pristine device. Their corresponding EL spectra under varying voltages are depicted in Supplementary Fig. 30. The efficiency improvement demonstrates the universality and effectiveness of our non-destructive post-treatment strategy.

For EtOH and BuOH, they both have good solubility for organic ammonium salts. Therefore, as shown in Supplementary Fig. 31-34, the EtOH post-treated devices exhibited peak EQEs of 0.65%, 0.42%, and 0.35% with sky-, pure-, and deep-blue emission, respectively. The BuOH post-treated devices showed EQEs of 1.65%, 1.11%, and 0.81% with sky-, pure-, and deep-blue emission, respectively. What's worse, both EtOH and BuOH post-treated devices feature poor EL spectral stability. This degraded overall device performance is attributed to the increased trap density caused by the erosion of the perovskite films by EtOH and BuOH, similar to the IPA post-treated devices. The inferior device performance generated by this method is similar to that reported in the reference mentioned by the reviewer (reference: Adv. Sci. 2022, 9, 2200073), which matches well with our findings and opinions.

For this issue, we have supplemented some discussion to enrich our work:

--- *“Apart from IPA and CF solvents, the S_N1 -like and S_N2 -like halide exchange mechanisms were validated by further expanding the solvent choices. The devices based on the post-treatment with other antisolvents, such as chlorobenzene (CB), toluene (Tol),*

and xylene (Xyl), also exhibited significantly improved device performance, as shown in Supplementary Fig. 29,30. This is attributed to the protective effect of these antisolvents on perovskite films. Similar to IPA, solvents such as ethanol (EtOH) and butanol (BuOH) feature the similar erosive effect on perovskite films, leading to distinctly degraded luminescence efficiency and EL spectral stability, as shown in Supplementary Fig. 31-34. In conclusion, by exploring the interaction between post-treatment solvents and perovskites, the solvent range can be further expanded for achieving desirable luminescent properties from perovskites.” (from Page 16, Line 22 to Page 17, Line 3)

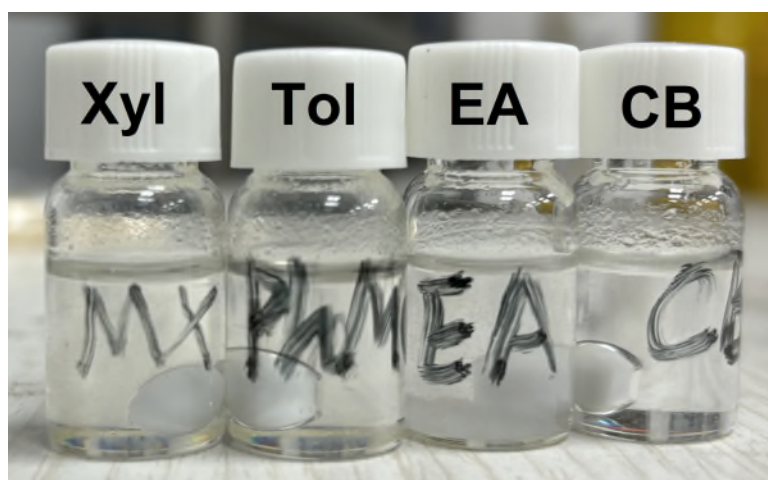
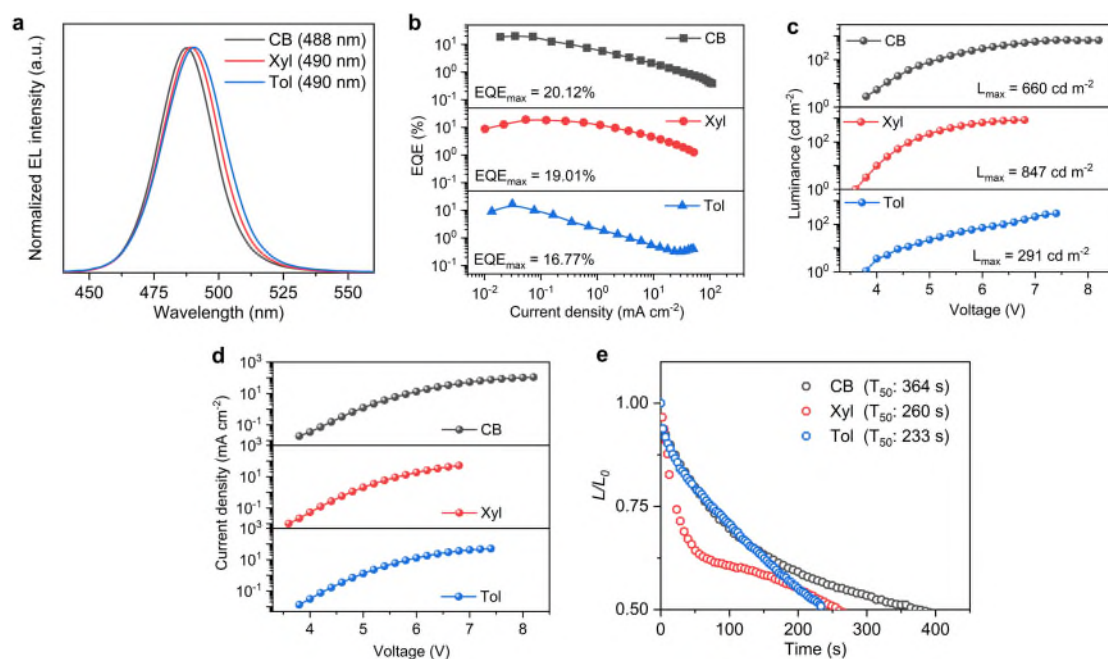
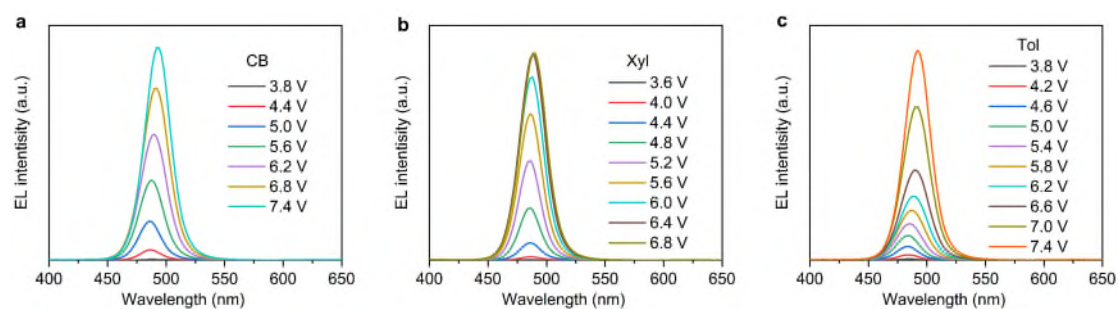


Fig. R3. Photograph of solubility of BACl in different solvents.



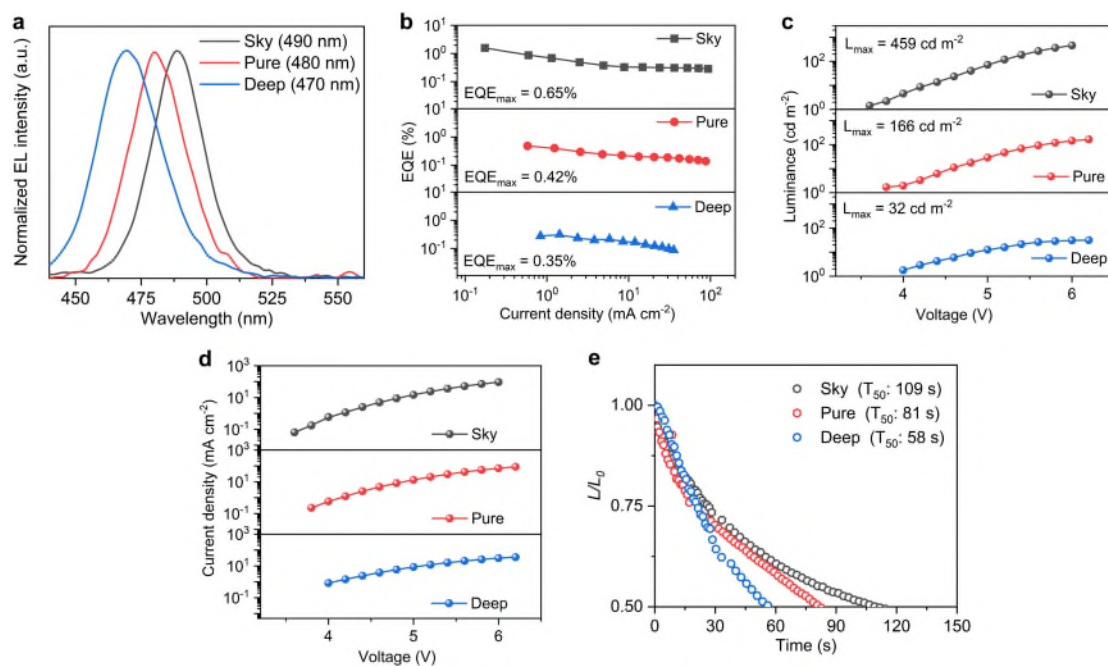
Supplementary Fig. 29. Device performance of Anti-solvent post-treated PeLEDs.

a Normalized EL spectra. **b** Dependence of the EQE versus current density. **c** L - V characteristic curves. **d** J - V characteristic curves. **e** Operational lifetime curves.

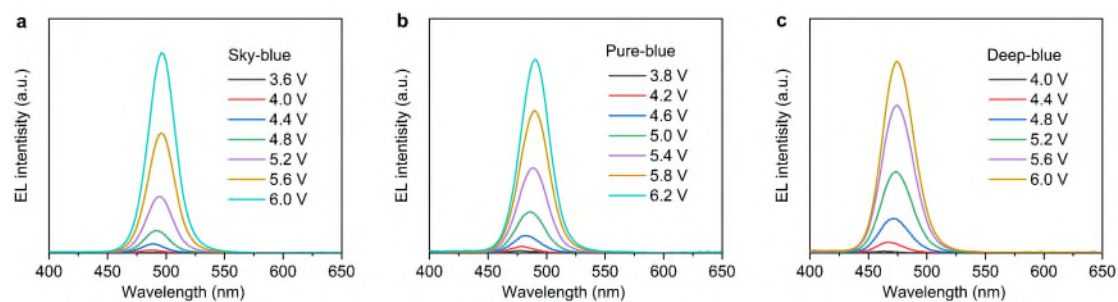


Supplementary Fig. 30. EL spectra with CF, Xyl, and Tol post-treatment under various driving voltages.

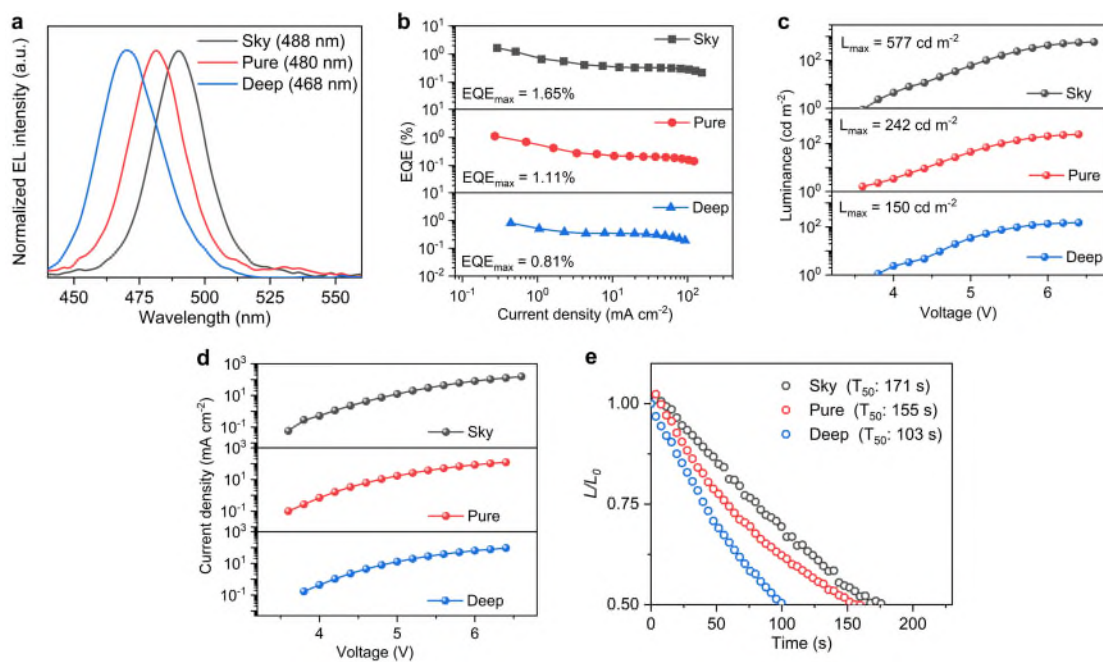
various driving voltages.



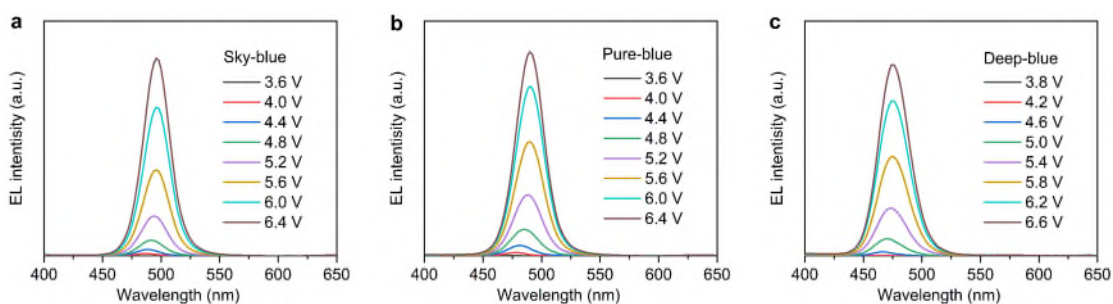
Supplementary Fig. 31. Device performance of EtOH post-treated PeLEDs. **a** Normalized EL spectra. **b** Dependence of the EQE versus current density. **c** L - V characteristic curves. **d** J - V characteristic curves. **e** Operational lifetime curves.



Supplementary Fig. 32. EL spectra of the sky-, pure-, and deep-blue devices with EtOH post-treatment under various driving voltages.



Supplementary Fig. 33. Device performance of BuOH post-treated PeLEDs. **a** Normalized EL spectra. **b** Dependence of the EQE versus current density. **c** L - V characteristic curves. **d** J - V characteristic curves. **e** Operational lifetime curves.



Supplementary Fig. 34. EL spectra of the sky-, pure-, and deep-blue devices with BuOH post-treatment under various driving voltages.

3. Comment (Reviewer #2): *It is necessary to show the UPS data and energy diagram of HTL (mixture of normal Al4083 aqueous solution and ETA) with different amounts of ETA such as 1,2,3,4,5,6,7,8,9,10 vol.%. Also please show the device performance differences (EQE, L_{max} , current density, operational lifespan, color stability (EL vs wavelength with different voltages)) of distinct HTL-based PeLEDs with different*

amounts of ETA from 1 to 10 vol.%.

Response: We thank the reviewer for suggesting us provide the UPS and device data based on the PEDOT:PSS with different ratios of ETA, which has certainly enriched our research. First of all, we feel sorry that the optimal ETA ratio was mismarked as 2 vol.% in the original manuscript. After carefully rechecking our experimental record, we confirm that our devices were fabricated by using the PEDOT:PSS solution with ETA ratio of 4 vol.%, which has been revised in the **Methods** section. We really apologize for our carelessness.

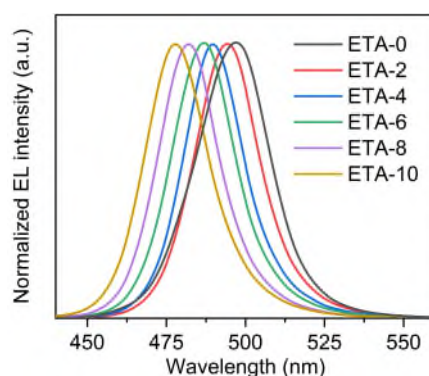
Reminded by the reviewer, we recognize that we ignored the energy level change of PEDOT:PSS films by ETA modification. Therefore, we retested the UPS spectra for PEDOT:PSS layers with different ratios of ETA (0, 2, 4, 6, 8, 10 vol.%), as shown in Supplementary Fig. 19 and 20. The HOMO level of the pristine PEDOT:PSS film is 5.2 eV, which is in agreement with that reported in literatures. After ETA modification, the HOMO levels are increased to a range between 5.62 eV and 5.74 eV, and the HOMO level of ETA-4 PEDOT:PSS layer in our study is 5.67 eV, which reduces the hole transport barrier from PEDOT:PSS to perovskite films.

Additionally, the determination of the optimal ETA ratio was based on the performance comparison of the pristine device at the initial stage. We tested the performance of the pristine PeLEDs with different ETA ratios (0, 2, 4, 6, 8, 10 vol.%), as shown in Supplementary Fig. 3 and 4. We found that when the ETA doping ratio was 4 vol.%, the device exhibited the best performance. The corresponding revisions are shown below:

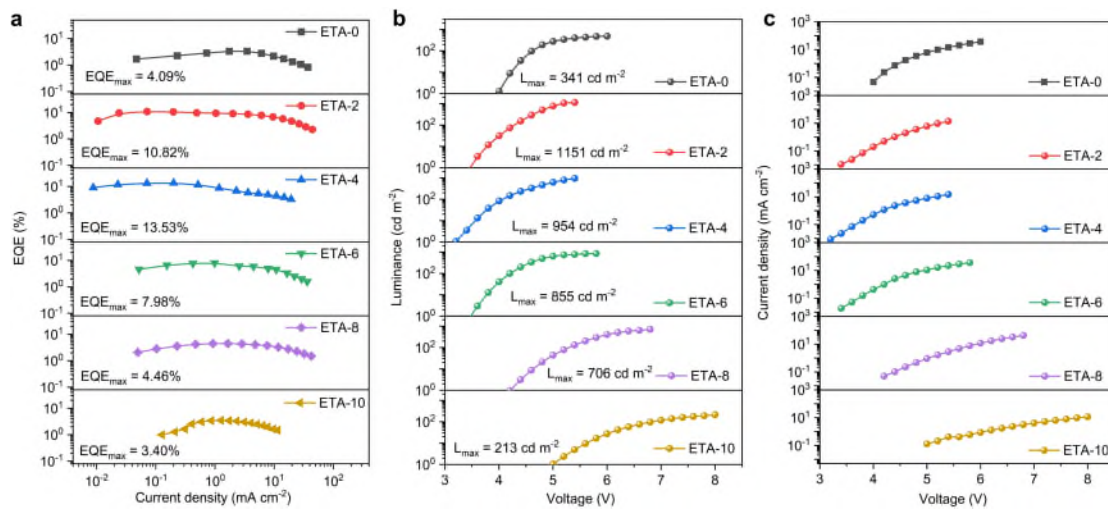
--- *“To examine the impact of different solvent post-treatment on the electroluminescence (EL) of perovskites, the corresponding PeLEDs with a structure of indium tin oxide (ITO)/PEDOT:PSS/perovskite/1,3,5-Tris(1-phenyl-1H-benzimidazol-*

2-yl)benzene (TPBi)/lithium fluoride (LiF)/aluminum (Al) were fabricated. The optimal ratio of the modifier ethanolamine (ETA) in PEDOT:PSS was first screened. By comparison, the device based on the PEDOT:PSS layer doped with ETA of 4 vol. % (denoted as ETA-4) exhibits the best performance, hence we selected ETA-4 as the hole transport layer for further investigation (Supplementary Fig. 3,4). Consistent with the PL results, the pristine device exhibits a sky-blue emission at 490 nm with an EQE_{max} of 13.53%, while the IPA-treated device shows a significantly lower EQE_{max} of 0.83% at 498 nm (Supplementary Fig. 5).” (Page 6, Line 9-20)

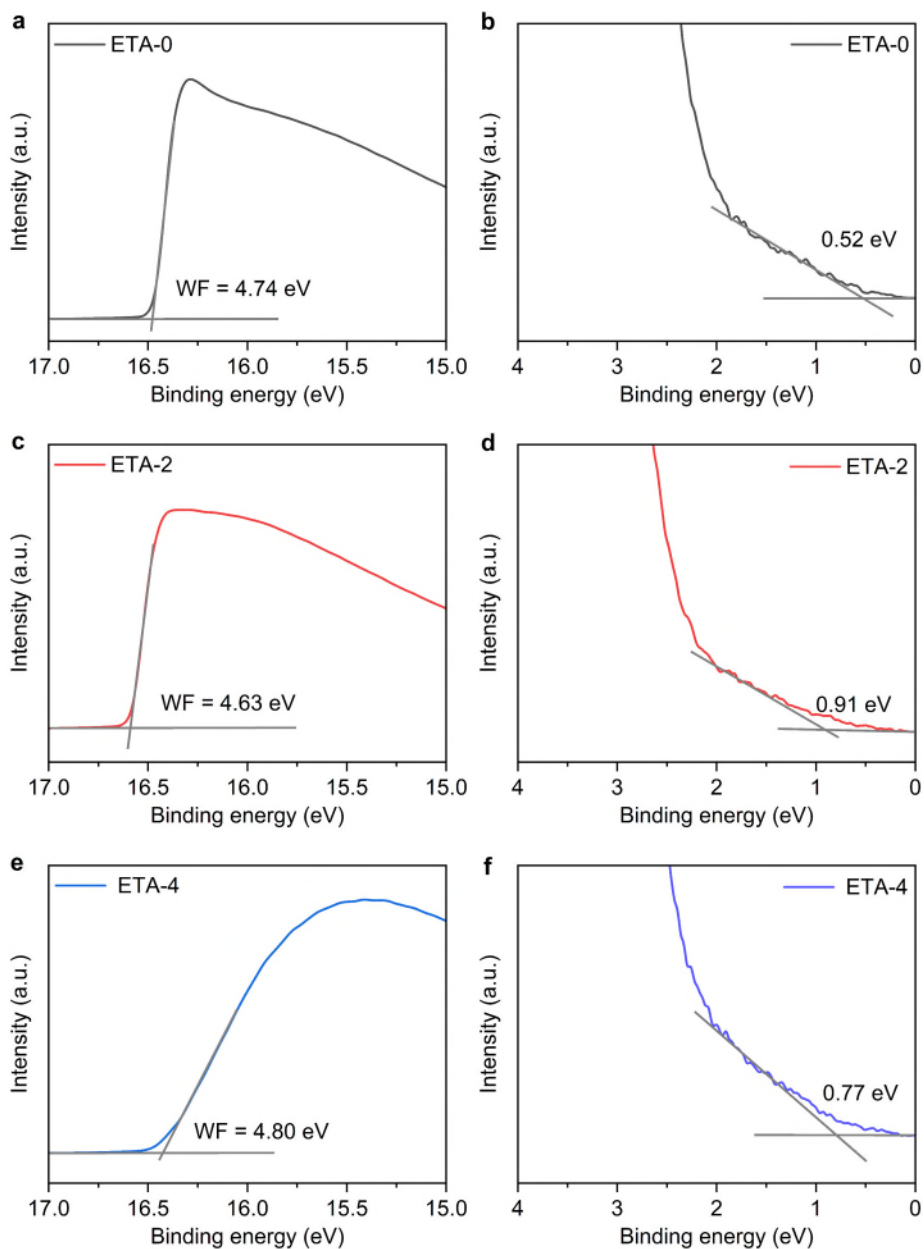
--- “The device energy level diagram is schematically depicted in Fig. 4a, where the valence and conduction bands of perovskite film were characterized through ultraviolet photoelectron spectroscopy (UPS) and Tauc plot analysis of the absorption spectra (Supplementary Fig. 17). The energy levels of PEDOT:PSS layers with varying ETA doping ratios were determined by the UPS spectra in Supplementary Fig. 19,20, indicating that ETA modification facilitates the hole transport by reducing the energy barrier from PEDOT:PSS to perovskite films.” (Page 14, Line 14-21)



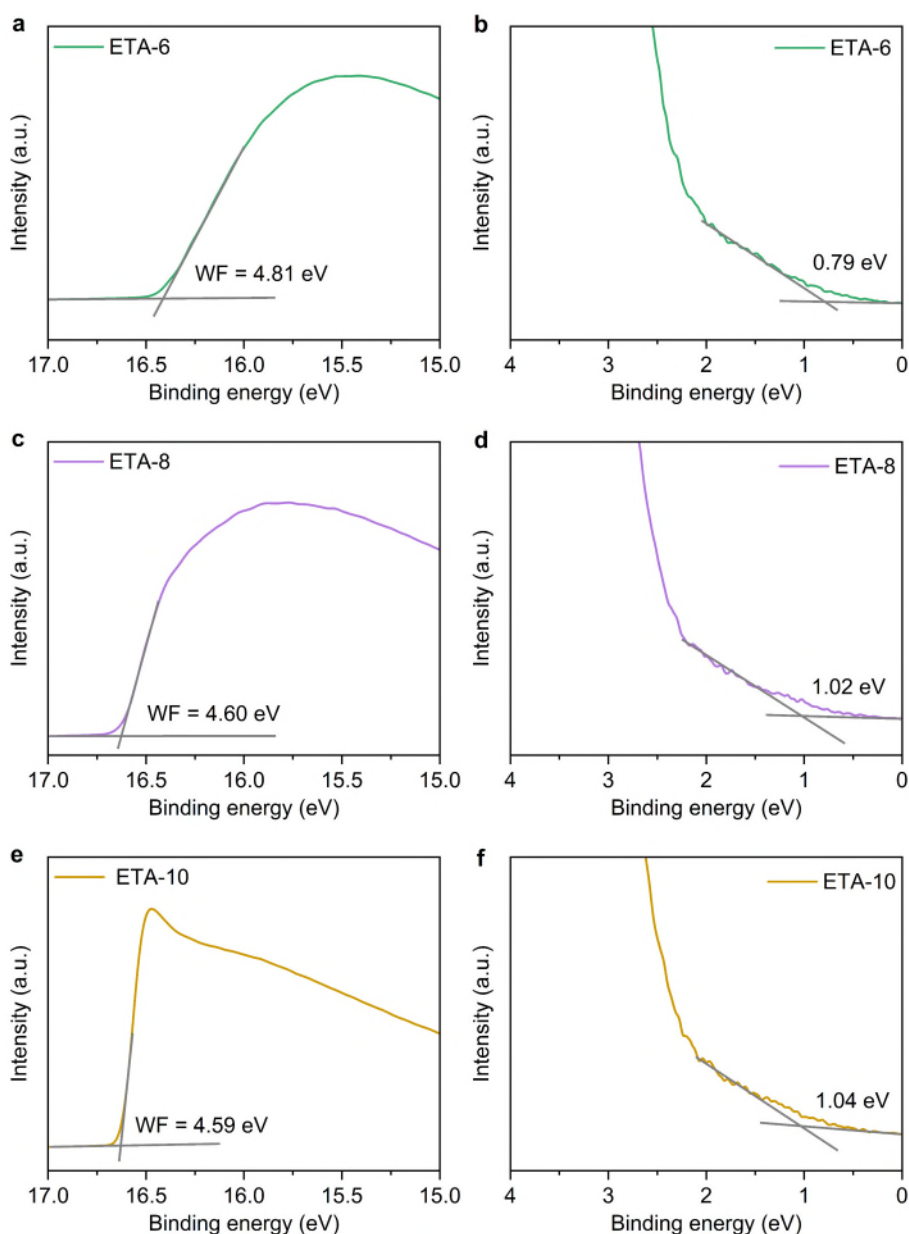
Supplementary Fig. 3. Normalized EL spectra of PeLEDs based on HTL layers with different ETA doping ratios (0, 2, 4, 6, 8, 10 vol.%).



Supplementary Fig. 4. EL characteristics of PeLEDs based on HTL layers with different ETA doping ratios (0, 2, 4, 6, 8, 10 vol.%). **a** Dependence of the EQE versus current density. **b** Luminance-voltage (L - V) characteristic curves. **c** Current density-voltage (J - V) characteristic curves.



Supplementary Fig. 19. UPS measurements of ETA-modified PEDOT:PSS films. **a, c, e** Secondary-electron cutoff regions in the UPS spectra of **(a)** ETA-0 (pristine PEDOT:PSS), **(c)** ETA-2, **(e)** and ETA-4 films. **b, d, f** Secondary-electron onset regions of **(b)** ETA-0 (PEDOT:PSS), **(d)** ETA-2, **(f)** and ETA-4 films.



Supplementary Fig. 20. UPS measurements of ETA-modified PEDOT:PSS films. **a, c, e** Secondary-electron cutoff regions in the UPS spectra of **(a)** ETA-6, **(c)** ETA-8, **(e)** and ETA-10 films. **b, d, f** Secondary-electron onset regions of **(b)** ETA-6, **(d)** ETA-8, **(f)** and ETA-10 films.

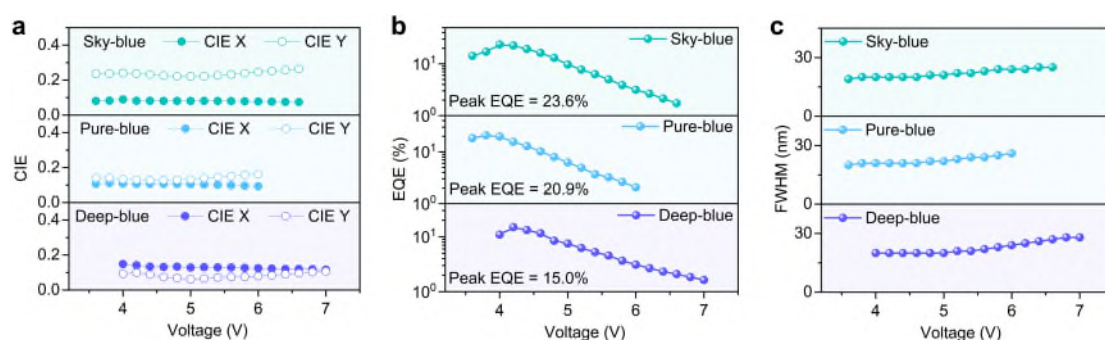
4. Comment (Reviewer #2): *In Fig. S21, it seems the emission wavelength has changed as operation voltage, so CIE coordination change plot for different operation voltages should be provided (CIE x,y coordinate vs voltage plot) Also, EQE and FWHM plot as*

a function of voltage should be denoted.

Response: We appreciate these suggestions. We have supplemented the relevant data, as shown in Supplementary Fig. 27. Due to the ionic property of perovskites, high current injection is prone to induce ion migration and thus causes slight redshift of blue emission.

One sentence has been revised on this issue:

--- “Additionally, the CF post-treated PeLEDs exhibit good spectral stability as evidenced by the slight EL spectral shift with increasing driven voltages, which is in accordance with their stable CIE coordinates (Supplementary Fig. 26,27).” (Page 16, Line 10-14)



Supplementary Fig. 27. Device performance of CF post-treated blue PeLEDs. **a** Dependence of the CIE coordinates versus voltage. **b** Dependence of the EQE versus voltage. **c** Dependence of the FWHM versus voltage.

5. Comment (Reviewer #2): The electrical explanation for the high efficiency should be described because there have been many papers showing higher PLQY but lower EQE compared to this paper.

Response: We thank the reviewer for the constructive suggestion for our work. According to classical LED model, the EQE is determined by three fundamental factors, which are internal quantum efficiency (IQE), charge transport balance factor, and

device light out-coupling efficiency. To unravel the reasons for the high efficiency of our devices, we will analyze these three factors one by one.

Firstly, IQE characterizes the luminescence performance of the emissive layer, which is defined as the ratio of generated photon number to the injected charge number. Generally, IQE is in positive correlation with the PLQY of emissive layer, but they are absolutely not the same parameter. IQE describes electrical excitation while PLQY comes from optical excitation. Different intensities and types of excitations yield distinct quantum efficiencies. This is one of the reasons for the contradiction between high PLQY and low EQE as many paper reports. For instance, many papers report high PLQYs around 100% while poor EQEs around 5%, which seems quite unreasonable. In our work, the CF post-treatment effectively improves the PLQYs of the blue perovskite films, providing a favorable precondition for high device efficiency.

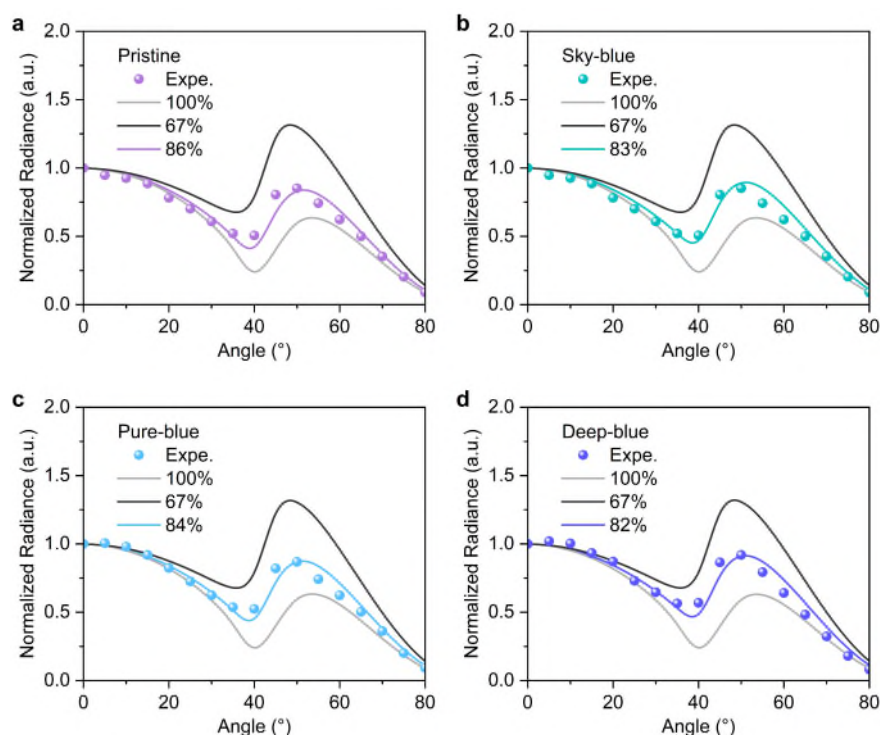
Secondly, improving the charge transport balance factor is also critical for high efficiency. As we have responded for Comment 3, the ETA modification, which is inspired by our previous works, has been demonstrated to reduce the charge transport barrier from HTL to perovskite layers, thereby facilitating the charge balance inside perovskite films and improve the recombination efficiency. The corresponding discussion has been added in our revised manuscript:

--- *“The device energy level diagram is schematically depicted in Fig. 4a, where the valence and conduction bands of perovskite film were characterized through ultraviolet photoelectron spectroscopy (UPS) and Tauc plot analysis of the absorption spectra (Supplementary Fig. 17). The energy levels of PEDOT:PSS layers with varying ETA doping ratios were determined by the UPS spectra in Supplementary Fig. 19,20, indicating that ETA modification facilitates the hole transport by reducing the energy*

barrier from PEDOT:PSS to perovskite films.” (Page 14, Line 14-21)

Thirdly, enhancing device light out-coupling promotes the light release from device inside to air. **In the following, we provide the discussion on light out-coupling to unravel the reasons for the high efficiency of our devices (also see in the response for Reviewer 1 # Comment 6):**

We first measured the horizontal transition dipole moments (TDMs) Θ of the perovskite films. As shown in Supplementary Fig. 22, the pristine perovskite film exhibits a high Θ value up to 86%, while the sky-, pure-, and deep-blue films feature the similar Θ values of 83%, 84%, and 82%, respectively. As widely reported, such high Θ is beneficial for improving the light extraction efficiency of devices, thereby improving the external quantum efficiencies of blue PeLEDs.



Supplementary Fig. 22. Horizontal transition dipole moments measurement of perovskite films. Angle-dependent PL measurements of (a) pristine (Θ : 86%), (b) sky-blue (Θ : 83%), (c) pure-blue (Θ : 84%), and (d) deep-blue (Θ : 82%) perovskite film.

The orientation of TDMs in the quasi-2D film is quantified as the ratio of horizontal TDMs, denoted by Θ .

Then, we utilized finite-difference time-domain (FDTD) simulation to qualitatively investigate the light out-coupling. According to conventional LED models, large portion of light is trapped inside device due to various channels of optical loss, such as waveguide mode, substrate mode, and metal surface plasmonic polaritons (SPP) mode. Importantly, the waveguide mode light loss is highly sensitive to the thickness of luminescent film. Reducing the thickness of perovskite film is favorable for mitigating the light waveguide. In our work, the thicknesses of blue perovskite films are less than 20 nm, which are much smaller than those of conventional LEDs, so we speculate that the light extraction efficiencies of our devices are higher than those of conventional LEDs. To demonstrate the advantage of perovskite thin film (~ 20 nm), we constructed device models based on the perovskite films with medium thickness (60 nm) and high thickness (100 nm) and simulate their light out-coupling by FDTD method (Fig. R2.). Apparently, for all the sky-, pure-, and deep-blue devices, reducing the thickness of perovskite films can effectively boost the light out-coupling from device inside to air. Therefore, based on improved PLQYs and charge transport, we can attribute the outstanding efficiency to the high device light out-coupling, which originates from the high horizontal transition dipole moments and small thicknesses of perovskite films. For this issue, we have supplemented some discussion:

--- *“It’s noteworthy that the high EQEs of these blue PeLEDs rely on the good horizontal dipole orientation of the perovskite films. By fitting the angle-dependent PL test data, the horizontal transition dipole moments (TDMs) Θ of sky-, pure-, and deep-blue perovskite films reaches 83%, 84%, and 82%, respectively, which is higher than*

those of ideally isotropic emitters (67%) (Supplementary Fig. 22). A higher Θ is favorable for light extraction from the internal perovskite films to air. Compared to 86% of the pristine film, the similar Θ values in the post-treated films support the reliability of the anti-solvent non-destructive post-treatment strategy. Moreover, the small thicknesses of perovskite films may suppress the waveguide light loss within devices, further boosting the device light out-coupling.” (Page 15, Line 13-22)

It's worth noting that the FDTD simulation come from the view of optical theory, which is intended to unveil the potential factor for the high efficiencies of our devices. The finding from the FDTD results doesn't mean that the perovskite films should be prepared as thin as possible for higher light out-coupling. Reducing the film thickness blindly is more likely to cause device current leakage under bias. Actually, the film coverage, phase distribution, and electrical property of perovskite film, which all have critical impact on the device performance, are highly related to perovskite film thickness.

In summary, high efficiency of PeLEDs requires the collaborative improvement of IQE, charge transport balance, and device light out-coupling. Only high PLQY does not guarantee high device efficiency.

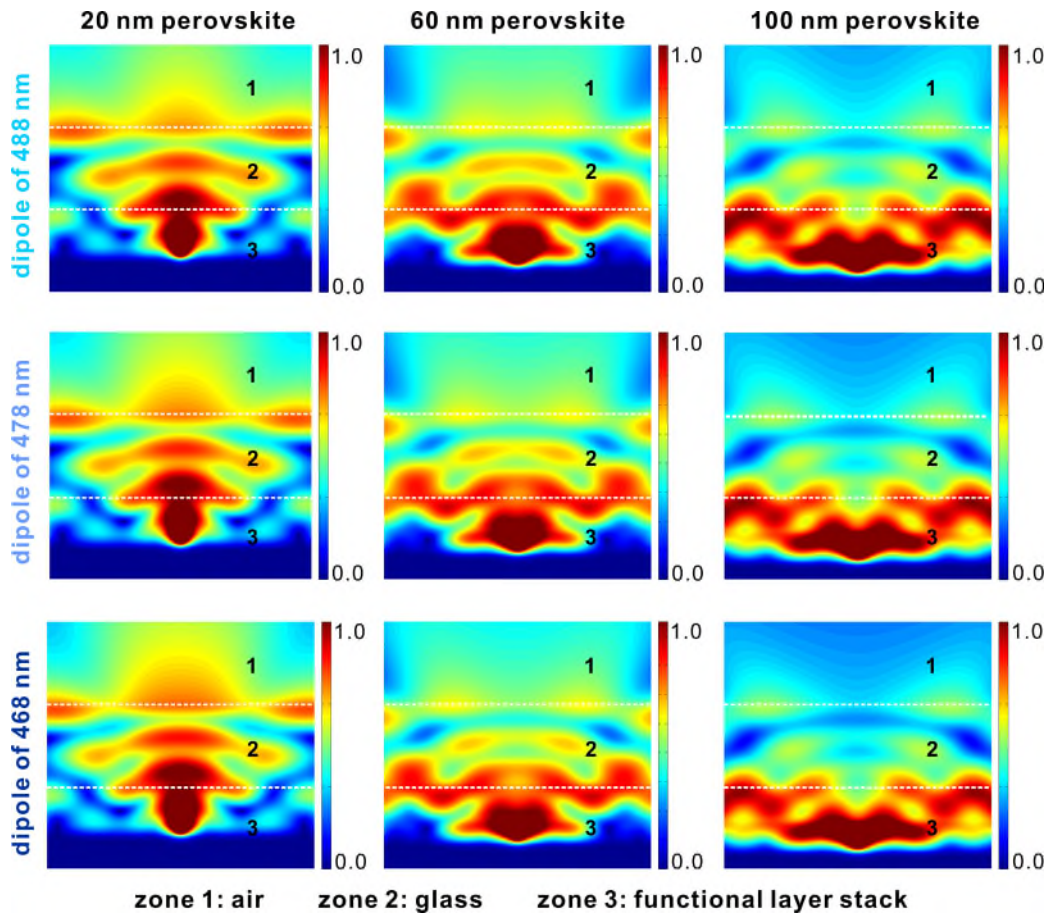


Fig. R2. FDTD simulations of sky-, pure-, and deep-blue PeLEDs based on perovskite films with the thicknesses of 20 nm, 60 nm, and 100 nm.

To Reviewer #3:

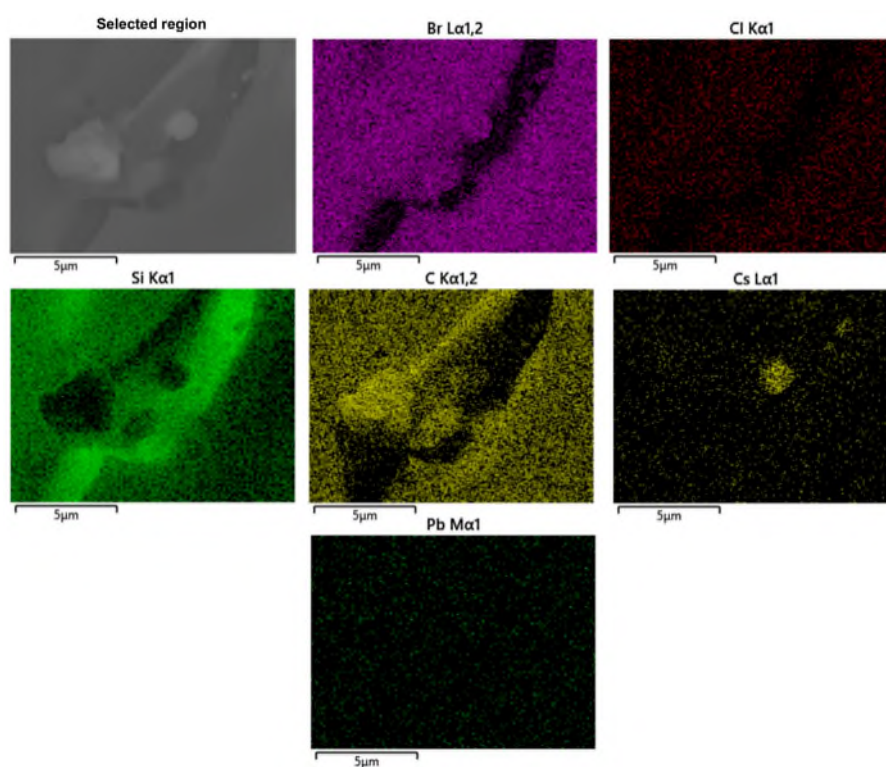
Blue perovskite light-emitting diodes (PeLEDs) continue to face significant challenges due to the difficulty in achieving high-quality mixed-halide perovskites with wide optical bandgaps. Traditional halide exchange methods, although effective in tuning the emission color of PeLEDs, often result in high defect densities due to solvent erosion. This study presents an innovative strategy for nondestructive in situ halide exchange, aiming to produce high-quality blue perovskites with low trap densities and tunable bandgaps. This paper is achieved through a chloroform post-treatment incorporating long alkyl chain chlorides. Both experimental results and theoretical calculations indicate a unique SN2-like ionic exchange mechanism with this approach. Unlike conventional halide exchange methods, this strategy not only modulates perovskite bandgaps but also prevents the formation of new halogen vacancies. The nondestructive halide exchange strategy enables the production of efficient PeLEDs across the blue spectral region, achieving record-breaking external quantum efficiencies of 23.6% (sky-blue emission at 488 nm), 20.9% (pure-blue emission at 478 nm), and 15.0% (deep-blue emission at 468 nm). This work represents a significant advancement in the field and provides valuable insights into halide exchange processes for developing high-performance blue PeLEDs.

Response: We thank the reviewer for the positive comments on our work. According to the reviewer's suggestions, we have carefully revised our manuscript. In the following, we provide the point-by-point response to the reviewer's comments and suggestions.

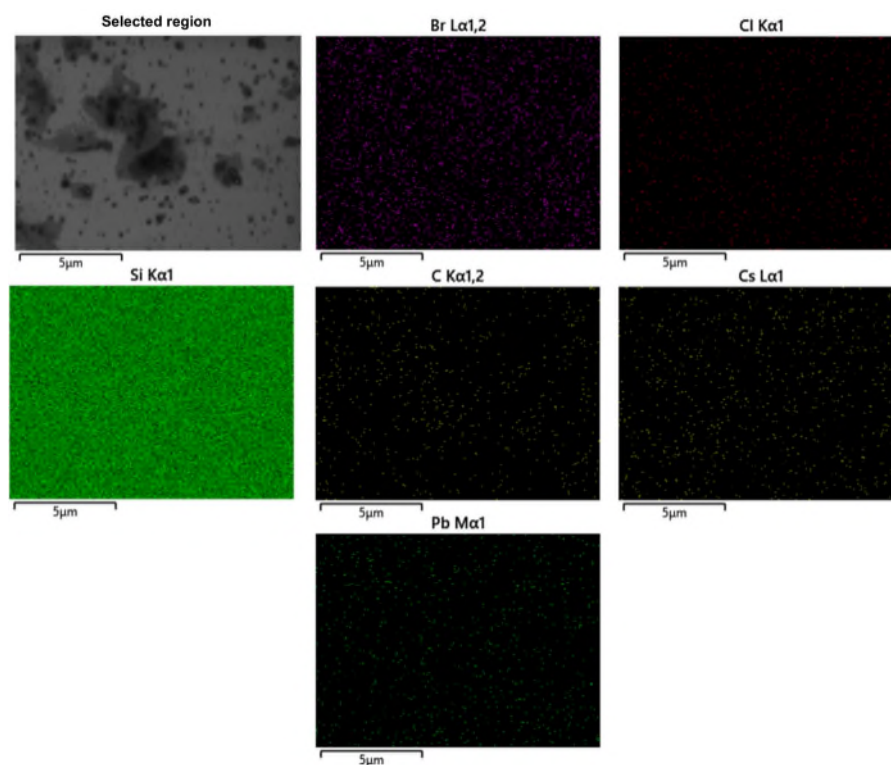
1. Comment (Reviewer #3): *It is mentioned that Cs and halogens are removed during IPA treatment, but the EDS data for Pb ions seems to be missing. Additionally, it would*

be better to compare figure S1 and S2 using the same scale bar for consistency.

Response: Thanks for the professional suggestions. We are really sorry for our carelessness. Accordingly, we have retested the EDS mapping with the same scale bar for both CF and IPA post-treatment (Supplementary Fig. 1,2). Notably, IPA can easily dissolve and remove some perovskite precursors such as CsCl, CsBr, and *p*-F-PEABr, so the signals from Cs and halogen elements are quite clear. However, the poor solubility of PbCl₂ and PbBr₂ in IPA makes it difficult to observe Pb signal. The corresponding discussion on this issue remains unchanged in our revised manuscript.



Supplementary Fig. 1. EDS mapping of the element components stripped from the perovskite films by IPA solvent post-treatment. The scale bar is 5 μm.

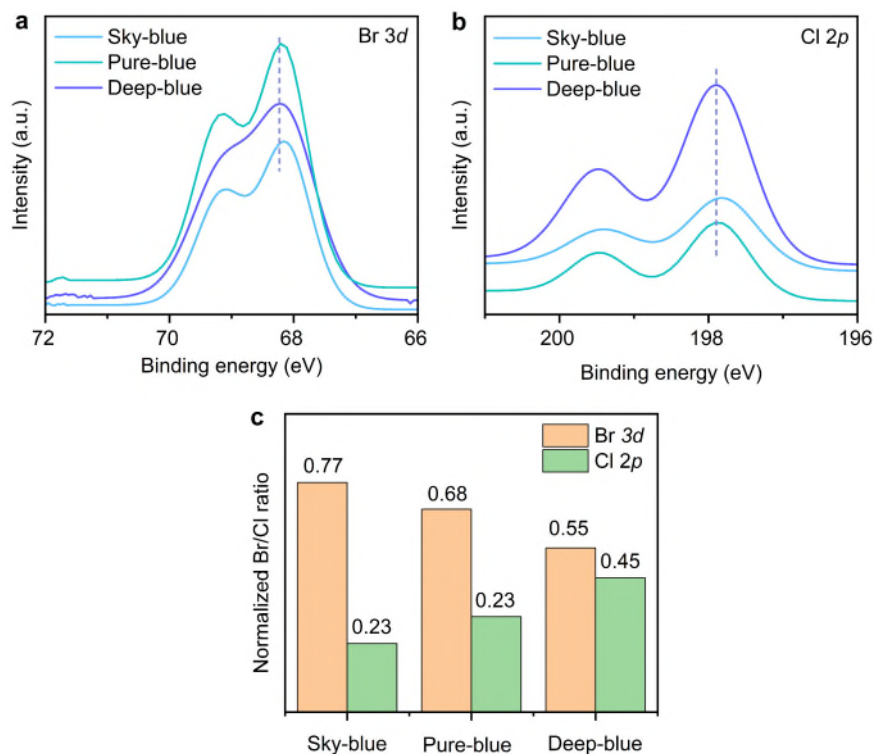


Supplementary Fig. 2. EDS mapping of the element components stripped from the perovskite films by CF solvent post-treatment. The scale bar is 5 μm .

2. Comment (Reviewer #3): *In Supplementary Fig 5, the XPS data shows inconsistencies in the peak intensity trends for Br and Cl depending on the wavelength of the light. The author needs more explain.*

Response: We thank the reviewer for suggesting us clarify the inconsistencies in the XPS peak intensity trends for Br and Cl. The inconsistency in the peak intensity trends of the XPS spectra arises from variations in signal strength during testing. Since we intended to compare the halogen ratio change after halogen exchange by XPS measurements, we don't need to pay attention to the absolute intensity variation. Instead, it is necessary to examine the relative intensity change between Br and Cl XPS peaks from the same sample, which were utilized to calculate the halogen ratios in different films by integrating the peak areas (Supplementary Table 2). To more intuitively

illustrate the changes in halogen ratios within these films, we have supplemented the corresponding halogen ratio chart, as shown in Supplementary Fig 7c. Apparently, smaller Br/Cl ratio corresponds to bluer perovskite film with wider bandgap.



Supplementary Fig. 7. a, b XPS spectra of (a) Br 3*d* and (b) Cl 2*p* from the perovskite films with BACl/BABr solution post-treatment. The inconsistency in the trend of peak intensities arises from variations in signal strength during testing. **c** Normalized Br/Cl ratios in the perovskite films with BACl/BABr solution post-treatment. The detailed process for calculating the absolute content of halogen atoms is provided in Supplementary Table 2.

Supplementary Table 2. Halogen ratios in the sky-, pure-, and deep-blue perovskite films obtained from the XPS measurements.

Area (Br)	n_{Br}	Area (Cl)	n_{Cl}	$n_{\text{Br/Cl}}$
-----------	-----------------	-----------	-----------------	--------------------

Sky-blue	6432	2264	1483	649	0.77/0.23
Pure-blue	4206	1481	1554	680	0.68/0.32
Deep-blue	6108	2150	3894	1704	0.55/0.45

3. Comment (Reviewer #3): *It is stated that a higher Cl ratio reduces defect tolerance; however, figure 3c shows that the V_{TFL} for deep blue is lower than that for pure blue. The author needs more explain.*

Response: We thank the reviewer for pointing out the error in the SCLC measurements. We feel sorry and admit that this contradiction results from the mislabeling of the fitting results of SCLC measurements. Accordingly, we have corrected the V_{TFL} for the deep-blue sample to 1.14 V, rather than 1.04 V. Besides, the trap state density in the deep-blue perovskite film has been recalculated. The corresponding figure and text have been corrected as shown below:

--- *“The initial trap-fill-limited voltage (V_{TFL}) decreases from 1.48 V of the pristine device to 0.97 V (sky-blue), 1.07 V (pure-blue), and 1.14 V (deep-blue) in the post-treated devices, indicating the lower trap densities in the post-treated perovskite films. Further evidence is provided by the trap density (N_t) quantitative calculations, where the trap state densities for the pristine, sky-, pure-, and deep-blue perovskite films are estimated to be 3.99×10^{18} , 2.61×10^{18} , 2.88×10^{18} , and $3.07 \times 10^{18} \text{ cm}^{-3}$, respectively.”*
(from Page 12, Line 22 to Page 13, Line 1)

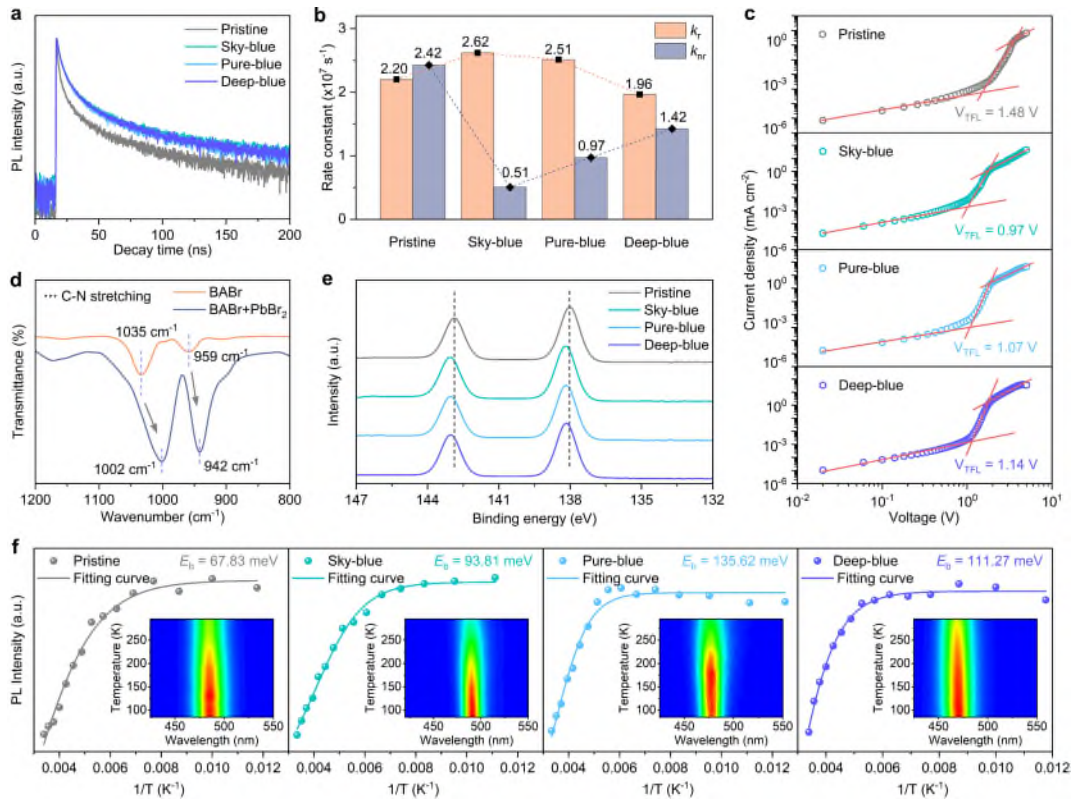


Fig. 3 Photophysical properties of blue perovskite films. **a** TRPL spectra of pristine and post-treated perovskite films. **b** Recombination rates derived from TRPL and PLQY results. **c** J - V curves of hole-only devices in SCLC measurements. **d** FTIR spectra of pure BABr and BABr/PbBr₂ mixture. **e** XPS spectra of Pb $4f$ core levels. **f** Relevant integration of the temperature-dependent PL intensity of perovskite films and fitting curves for E_b . Inset is the corresponding temperature-dependent PL spectra.

4. Comment (Reviewer #3): *There are discrepancies between the figures mentioned in the paper and the corresponding descriptions. Please correct these, particularly the reference on line 176 (supplementary fig 2a -> fig 2a) and on line 271 (Supplementary Note 2 -> Supplementary Note 1).*

Response: We appreciate the reviewer's kind reminder. Accordingly, we have corrected these errors and carefully rechecked the manuscript to avoid similar errors.

--- "As depicted in Fig. 2a, the halide exchange proceeding in conventional IPA-based

treatment involves two sequential steps, similar to the S_N1 nucleophilic substitution in organic reactions.”

--- “ $PLQY = k_r/(k_r + k_{nr})$ and $\tau_{average} = 1/(k_r + k_{nr})$, where k_r and k_{nr} represent the radiative and nonradiative recombination constants (Supplementary Note 1), respectively.”

5. Comment (Reviewer #3): *In figure 3(d), it is stated that the shift of the C-N peak in FTIR data is contributed by the coordination interaction between the amine group and the uncoordinated Pb atoms. Given that the amine group of ligands is generally attached to halides of the perovskite frame by coulombic attraction, is there a reason to describe the interaction between the amine group and Pb atoms?*

Response: We thank the reviewer for the insightful comment and question. We strongly agree with the reviewer that the amine groups of most ligands interact with the halogens on the crystal surface through coulombic attraction. However, halogen vacancies are inevitably present at perovskite grain boundaries, allowing the N atoms in the amine groups to interact with Pb atoms via lone pair electrons. This interaction helps reduce the trap states in perovskite films, which has been reported in many studies (e.g., Nat. Photon. 2024, 18, 425-431; Nature 2023, 615, 830-835; Adv. Funct. Mater. 2021, 31, 2005553). Therefore, we investigate the interaction between the amine group and Pb atoms to demonstrate the defect passivation effect of our strategy.